Technical Report
Report No.: 2019/19

METHODS FOR PREDICTION OF THERMALLY-INDUCED ICE LOADS ON DAMS AND HYDRO-ELECTRICAL STRUCTURES

Literature review

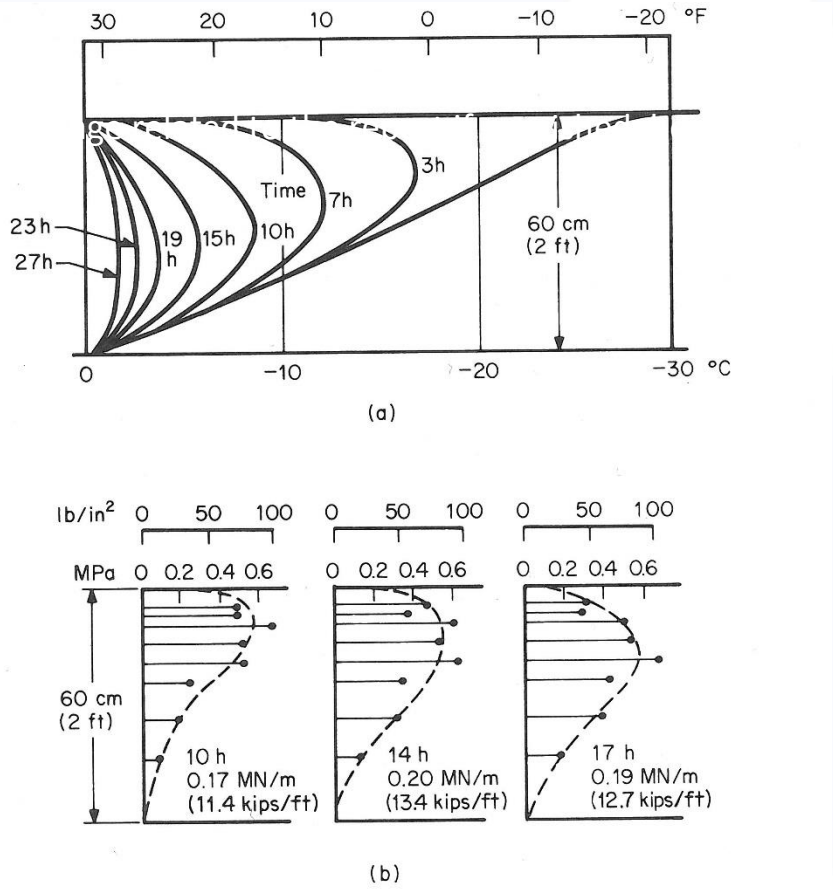

Irina Sæther

P.O.BOX 250
N-8504, NARVIK, NORWAY
PHONE: +47 76 96 53 50, FAX: +47 76 96 53 51
info@tek.norut.no
www.norut.no/narvik_en

norut
NORTHERN RESEARCH INSTITUTE
NARVIK

Contracting institution:	Contracting Ref:	ISBN:
Author(s):	Project No.: 3014.03	ISSN:
Author 1 Irina Sæther	Document Type: Technical report	Pages: 57
Author 2	Document No.:	Version no.: 2
Author 3	Date: 28 04 2019	Reviewed by: Christian Petrich
Author 4	Status/Availability: Open	Technical Responsible: Bård Arntsen

Document title:

Methods for prediction of thermally-induced ice loads on dams and hydro-electrical structures

Abstract/Summary:

Recommended values of the thermally-induced loads at different locations and climatic zones were primarily obtained on the basis of available empirical values. A review of the literature on the theories and analytical models previously proposed for calculation of the thermally-induced loads on dams and other hydro-electrical structures is presented in this report.

The comparison of previously proposed models with measured data showed a wide variation, and none of the available models for predicting ice pressure were capable of predicting the measured pressure within an acceptable margin of error. In Norway, the values of the thermal ice load are suggested to vary between 100 and 150 kN/m. In other countries, such as Canada and USA, the recommended thermal ice loads are higher than in Norway and varies between 150 and 220 kN/m. The maximum thermal ice load measured during laboratory experiment in Sweden was 250 kN/m.

This literature study focuses also on current standards and recommendations, in Norway, Sweden, Canada, USA and Russia, for determining thermal ice pressure acting on dams and reservoirs, i.e. methods for the thermally-induced loads or recommended values for an equivalent line load representing the thermal ice pressure.

Keywords:

thermally-induced ice loads, ice pressure, dams

Notices:

Distribution:

Preface

The main goal of the ICEDAM (Ice forces on the dams) project carried out at Norut Narvik during the period 2011-2014, is to further develop and improve models for the calculation of ice forces on dam structures and thus contribute to sustainable energy production in Norway. The main objective of the ICEDAM project is to ensure dam safety and to ensure that any enhancement measures are implemented where necessary.

As the first phase of the project a literature survey to identify what has previously been made regarding the calculation of thermally-induced ice forces on structures, are completed and presented in this report. The literature study includes the current rules and guidelines for the calculation of ice load in both Norwegian and international norms and guidelines and description of existing analytical, semi-empirical methods for calculating thermally-induced ice forces. The presented literature study is intended to contribute as a basis for further work in the project.

Contents

1. Introduction

The gravity dams are solid concrete structures that maintain their stability against design loads from the geometric shape and the mass and strength of the concrete. Generally, they are constructed on a straight axis, but may be slightly curved or angled to accommodate the specific site conditions. A dam must be designed with a high factor of safety to withstand the designed loads.

Analysis of the stability and calculation of the stresses are generally conducted at the dam base and at selected planes within the structure. If plane of weakness exist in the foundation, they should also be analysed.

The basic stability requirements for a gravity dam for all conditions of loading are that:

- It must be safe against overturning at any horizontal plane within the structure, at the base, or at a plane below the base.
- It must be safe against sliding on any horizontal or near-horizontal plane within the structure at the base or on any rock seam in the foundation.
- The allowable unit stresses in the concrete or in the foundation material shall not be exceeded.

Characteristic locations within the dam in which a stability criteria check should be considered include planes where there are dam section changes and high concentrated loads. Large galleries and openings within the structure and upstream and downstream slope transitions are specific areas for consideration.

There are two types of loads act on the dam: stabilizing loads (weight of the dam and weight of water over dam section) and overturning loads (water pressure, uplift pressure, ice pressure). The silt pressure, wave pressure and earthquake pressure may also contribute to the overturning loads. Figure 1 presents the most common static loads used in the stability analysis and stress calculations. Various loads may act on the body of the dam but all these loads seldom act simultaneously on the dam. Therefore, design of the dam should be based on the most adverse combination of probable loading conditions.

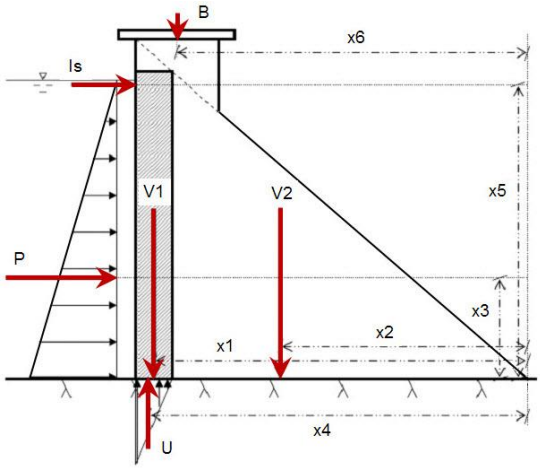

Figure 1. Some of the stabilizing loads and overturning loads acting of the buttressed dam: V1, V2 and B are weights of the dam section and the bridges; P is the headwater pressure; U is the uplift pressure and Is is ice pressure (Norut Narvik report 2009).

Static loads acting on the body of the dam can be described as following:

Weight of the dam: Weight of the dam is the most important stabilizing load action on the dam. The loads act in the downward direction at the centre of the gravity of the dam sections. The weight of the structure includes the weight of concrete of section and other installations on the dam. The weight of the dam section is determined by multiplying the area of the cross section with the unit of weight of the material of the dam.

Water pressure acting on a sloping face of the dam body can be decomposed into a horizontal and a vertical component.

Weight of water over dam section (vertical component of the water pressure): Weight of the columns of water standing over the sloping faces of the dam act as stabilizing loads. These loads act the downward direction at the centre of the gravity of the columns.

*Water pressure (vertical component of the water pressure)*A dam is subjected to water pressure due to water standing against it. The headwater pressure acts on the downstream direction whereas the tail water pressure acts in the downstream direction.

Head water pressure acting on the upstream face of the dam is equal to the area of the load triangle and given by:

$$P = \frac{1}{2} wh^2 \quad (1)$$

where h is depth of water standing against the dam and w is unit weight of water.

The centre of application of the load is located at the centre of the gravity of the triangle which 1/3 of the depth of the water from the base.

Tail water pressure acting on the downstream sections of the dam is simultaneous to the head water pressure and it acts at the point 1/3 of the depth of the water from the base.

Uplift pressure (pore pressure): Water that seeps through the pores of the material of the dam and foundation causes pressure under the dam foundation in the upward direction. This results in the reduction of the stabilizing loads on the base. Intensity of uplift pressure is maximum at the upstream heal of the dam base and goes on reducing to the downstream toe. Intensity of uplift pressure at the upstream is taken equal to the hydrostatic pressure at the heal and the pressure at the downstream is taken as equal to hydrostatic pressure of water at the toe. The uplift pressure varies in a straight line between heal and toe as shown in Figure 1. The uplift pressure acts in an upwards direction at the centre of gravity of the pressure diagram. In order to reduce uplift pressure, drainage galleries are provided in the body of the dam.

Ice pressure/ice loads: Ice pressure can produce a significant load against the face of a dam in locations where winter temperatures are cold enough to cause a relatively thick ice cover. Ice pressure is created by thermal

expansion of the ice and by wind drag, but it is not fully known as to how much pressure is exerted by the sheet of ice on the dam face. Several design codes are available to help in design. According to these codes the ice pressure acts along the length of the dam at a height below or at the water level. The magnitude of this load varies much in different codes. When the stability of a dam is considered, an equivalent line load represents the thermal ice pressure acting on the face of the dam.

The following ice loads on dams or other structures should be considered during the design or reconstruction phases:

− Horizontal load due to temperature fluctuation in a stable ice cover (thermal ice load).
− Horizontal load from moving ice floes (dynamic load).
− Vertical forces from a stable ice cover subject to water level fluctuations.

Ice expands with increasing temperature, and vice versa. However, unlike other materials, water expands when it changes phase from liquid to solid. These two properties, along with the creep properties of ice, explain the forces that develop when ice undergoes a temperature change. The temperature of ice changes because of conduction, radiation, and convection heat transfer at its surface. The depth to which temperature changes take place depends on the thickness of the ice cover, the presence or absence of snow on its top surface, and the environmental conditions (Michel 1970, 1978; Sanderson 1988).

A very thin ice sheet has a temperature close to 0°C. As the sheet grows in thickness, the temperature of its top surface decreases because of the low air temperature. The upper layer of the ice contract, but since the temperature lower boundary is still 0°C the contraction causes tension, creep of ice and cracks in the upper layers of the ice. The ice cover usually grows slowly. Except for the first few centimeters of growth, the ice has time to creep without the formation of the tensile cracks as long as the temperature at the upper surface is constant (Ashton 1986). If, however, the air temperature suddenly falls considerably, the upper surface of the ice assumes a new temperature, and after some time a steady state thermal gradient will be established in the ice cover. The upper surface contracts rapidly, but the lower boundary stays approximately the same since its temperature stays at the freezing point.

The ice is floating on a horizontal water surface, so the free bending of the ice cover is restricted. Instead, the effect is a bending moment in the cover, and the stresses are mostly released by the formation of deep cracks (Figure 2). If the change of temperature is very slow, the ice may deform viscously without formation of the cracks (Bergdahl 1978).

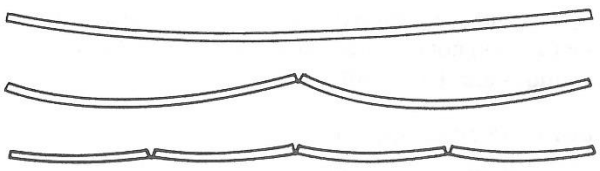

Figure 2. Bending and cracking of a floating ice cover due to rapidly change of temperature at the upper surface (Bergdahl 1978, Ashton 1986).

Later if the ice cover is warmed up due to mild weather or water finding its way on to the ice, the upper layers will again expand. Pressure will develop in the ice and may be followed by shoving onto a beach or folding of the ice cover against banks and in zones of weakness (Figure 3).

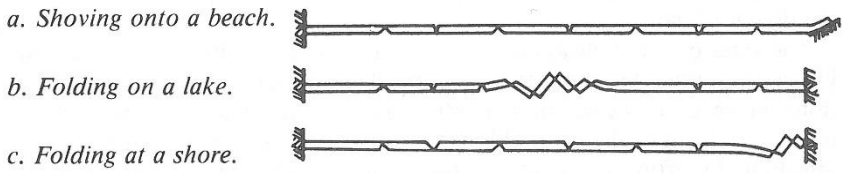

Figure 3. Examples of expanding ice covers (Bergdahl 1978, Ashton 1986).

In summary, factors influencing thermal ice loads (Engineering and Design - Ice Engineering 2002) are:

- The magnitude and the rate of change in the temperature.
- Heat transfer at the top surface and in the ice sheet; the ice coefficient of thermal expansion.
- Restrictions to expansion along the boundaries.
- Creep properties of the ice cover.
- Dry, wet and wide cracks in the ice cover, see Metge (1976), Kjeldgaard and Carstens (1980), Fransson (1988).
- The thickness of the ice cover and snow cover.
- Mechanical properties to ice.

Thermal ice load shall only be considered in lakes and in brackish seas and not in the open sea with saline water. Vertical ice loads may occur particularly where the water level initially remains at one level long enough for the ice to adfreeze to the structure, and then changes. As the later level changes, either the adfreezing bond developed between the ice sheet and the structure or the bending strength of the ice must be exceeded in order for the ice to move. Horizontal loads from moving ice floes are not going to be considered in the present report.

2. Previously proposed theories and models

Several theories have been proposed for estimating the thermal ice loads and ice pressures and have been reviewed by several authors (Engineering and Design - Ice Engineering 2002). A number of laboratory experiments and full-scale observations have been conducted to verify these theories. Most extensive reviews may be found in the following sources: Michel (1970), Bergdahl (1978), Kjeldgaard and Carstens (1980), Fransson (1988) and Hassan (1991).

The basis for the calculation of the stress in the ice can be a rheological equation where the rate of strain is given as a function of stress and the rate of change of stress. The rate of strain is a function of the rate of change of ice temperature. So, the first step towards the estimation of thermal ice pressures is calculation of the ice temperature or its derivative. The temperature calculations in details can be found in Bergdahl (1978). Basic rheological models of ice which have stress-strain-time characteristics similar to deformable solids and, thus mentioned later in this section, are well described by Mellor (1983). Some of the methods and analytical

theories that have been proposed for calculation of the thermal loads are presented below in this report. However, in spite of a number of analytical and numerical studies of ice loads, Gebre et al. (2013) asserted that general models for the estimation of ice loads are still not fully verified and accepted and concluded that there is a need for research to develop and validate numerical ice load models.

2.1. Royen (1922)

Royen (1922) proposed a simple analytical expression of the maximum pressure as a function of initial temperature and the rate of the temperature rise. Royen realized that, unlike most construction material, ice is a highly time-dependent material. To obtain a useful formula for thermal ice pressure, Royen compared creep curves by Hess (1902), Kreuger (1921) and from the own investigation at constant stress (700-900 kPa) and constant temperatures (-8 - 0 °C), see Figure 4.

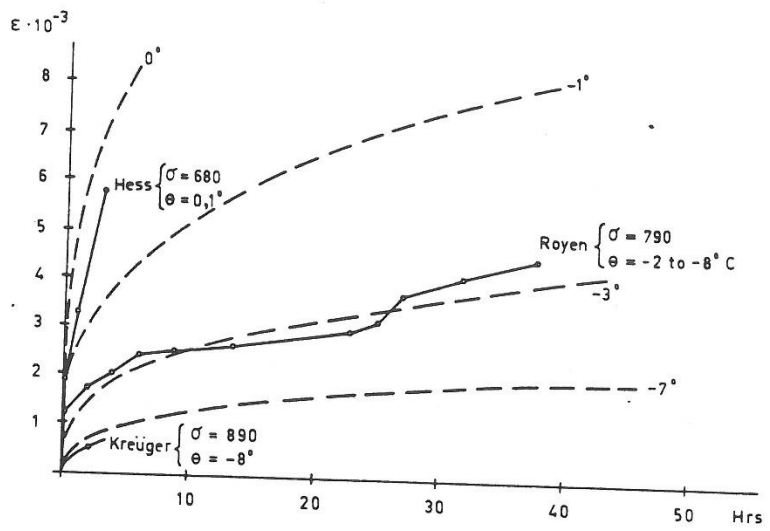

Figure 4. Experimental creep curves on lake ice and single crystals compared with Royen's formula with (after Royen 1922); from Fransson (1988).

In this stress interval Royen suggested the creep law:

$$\varepsilon(t) = k_1 \cdot t^q \tag{2}$$

where $\varepsilon(t)$ is a strain function of the time t (hours). In Eq. (2), k_1 and $q = 1/3$ parameters are used in Royen 's investigation.

The temperature dependence of the creep was established using experimental results from indentation tests at -35 °C to 0°C. Royen suggested that:

$$\varepsilon(\Theta) = \frac{k_2}{T_1 + |T|} \tag{3}$$

where k_2 and T_1 are constants; $T_1 = +1$ °C in the Royen's investigation and $|T|$ is the temperature (without sign). The stress dependence of the creep could not be established with ice data known to Royen. He suggested the linear relation, somewhat contradictory to later research (Fransson 1988):

$$\varepsilon(\sigma) = k_3 \sigma \tag{4}$$

where k_3 is constant.

Further, the stress-strain relation, obtained by combination of the three empirical equations, was presented by Royen as:

$$\varepsilon = \frac{c \cdot \sigma \cdot t^{1/3}}{1 + T} \tag{5}$$

where ε is compressive strain; σ is applied stress (≤ 800 kPa); t is loading time (hours); T is ice temperature (≤ 0 °C) and $6 \cdot 10^{-4} < c < 9 \cdot 10^{-5}$ (*°C cm²/(kph^1/3)*).

The non-restricted thermal expansion of ice can be written as:

$$\frac{d\varepsilon}{dt} = \alpha \frac{dT}{dt} \tag{6}$$

Royen differentiated Eq. (5) with respect to t keeping T and σ constant and equated the results with that of Eq. (6) :

$$\sigma = \frac{3\alpha}{c}(T+1)t^{2/3}\frac{dT}{dt} \tag{7}$$

But the act is a violation of the rules of differentiation as both σ and T are used as function of time, see below. Royen justified the approximation by its agreement with experimental values. Further, it was assumed that the temperature increase is linear in time:

$$T(t) = T_i - \dot{T} \cdot t \tag{8}$$

where $T(t)$ is mean temperature of ice (absolute value, °C); T_i is initial mean temperature of ice (absolute value, °C) and $\dot{T}$ is the constant mean temperature increase (*°C /h*).

By means of the equations Royen has found the maximum stress development (in kp/cm^2) during a temperature increase:

$$\sigma_{\max} = 0.9772\frac{\alpha}{c}(T_i+1)\sqrt[3]{\dot{T}(T_i+1)^2} \quad (9)$$

at the time (hours):

$$t_{\max} = 5\dot{T}/(2(T_i+1)) \quad (10)$$

With $\alpha = 5.5\cdot 10^{-5}$ °C and $c = 6\cdot 10^{-4}$ the standard form of the Royen's equation becomes:

$$P_{\max} = 0.9h(T_i+1)\sqrt[3]{\dot{T}(T_i+1)^2} \quad (11)$$

where $P_{\max}$ is force (t/m) and *h* is ice cover thickness (m).

A number of drawbacks in Royen's theory can be mentioned, for instance:

- The relation in the Eq. (5) had been found by test with paraffin wax which does not simulate the properties of fresh ice. The relation was based mainly on testes with lake ice. Both of these relations give an inadequate description of the behaviour of fresh water ice (Kjeldgaard and Carstens 1980).
- The elastic deformation of ice was ignored.
- No distinctions are made between different creep states of ice.
- The difference between uniaxial and biaxial load cases was not discussed.
- Because the temperature is assumed to occur uniformly over the ice thickness, the maximum ice pressure will be proportional to the ice thickness.

Later, a mistake made by Royen (1922) was corrected by Proskourjakov (1967). Royen had only made a partial derivation of Eq. (5) instead of a total derivation as σ and T varies with time. The result of this correction is that the final expression for the maximum pressure is divided by three. But the coefficients c and q were still empirical constants.

2.2. Brown and Clarke (1932)

Results from two experiments reported by Brown and Clarke (1932), ice cubes were subject to a temperature rise that was intended to be linear with time while two opposite cube faces were loaded exactly as much as needed to avoid an expansion in that direction. The results of the experiments were a few (three) points on a graph showing the temperature increase rate versus load increase rate, see Figure 5. As is seen the results are few and furthermore the experimental equipment was not able to realize the intended test conditions with any high degree of accuracy.

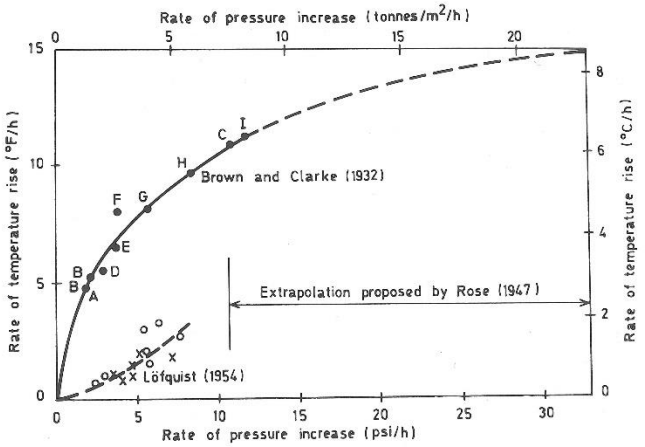

Figure 5. Relation between temperature rise per hour and pressure rise per hour (Brown and Clarke 1932); from Bergdahl (1978).

The continuous curve is the curve of Brown and Clarke 1932; filled circles A-C original point and D-I from shorter parts of the same experiments. The lower circles, crosses and dashed curve are from the experiments of Löfquist (1954).

2.3. Rose (1947)

Using the experimental data obtained by Brown and Clarke (1932), Rose (1947) generated curves to predict ice pressure. Rose's main contribution to the ice pressure problem was that he showed how the temperature distribution will develop in an ice cover that is subjected to a linear temperature rise at the top.

The computation of the ice forces were carried out by first using finite difference integration of the heat conduction equation to give the rate of change of temperature at a certain level in the ice cover. The presented curves illustrated pressures from 0 to 1.3 m for three distinct temperatures rise (5, 10 and 15 °F/hour). The curves were given for cases with and without effects of solar energy, and with and without lateral constraint. One of Rose's figures is shown in Figure 6.

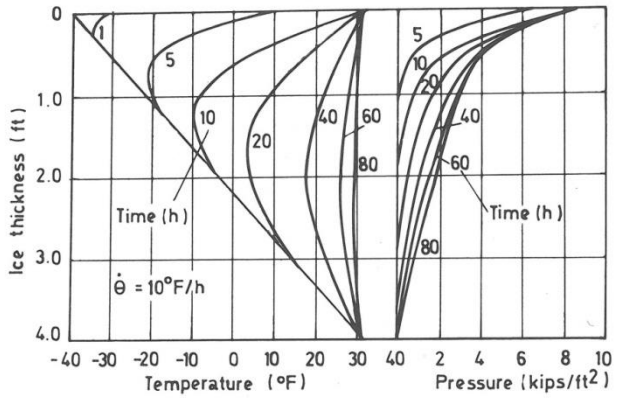

Figure 6. Ice temperature curves and resulting ice pressure curves (Rose 1947).

The inputs in the calculations are only ice thickness, rate of the temperature increase, the presence or absence of lateral constraints, and the presentence or absents of solar absorptions. No account was taken of the initial temperature.

2.4. Monfore (1947-1954)

The intention of their study was to determinate the thermal ice pressure on some dams in Colorado. Both in situ measurements of the ice pressure and the laboratory investigations of the creep properties of natural ice were conducted by Monfore (1954). The laboratory investigations by Monfore were made in almost the same way as Brown and Clarke. Small cylindrical ice samples were taken from two reservoirs, where ice cover thickness was approximately 45 cm and cut in such way that the axis of the cylinders was parallel to the ice cover surface. A meter in direct contact with the sample measured the axial strain. The temperature of the ice sample was controlled by means of cold air-circulation and the ice temperature was measured both at the periphery of the ice sample and at the axis.

Before a test was made the sample was kept at one of the following initial temperatures - 30°C, -20°C, -10°C, 0°C, 10°C, 20°C. Then the circulation of air was changed in such way that the temperature of ice was made to increase with one of the following rates: 2, 5, 10, 15 °F/hour. During the first 30 minutes the load was adjusted to give zero total strain every 5 minutes. Thereafter adjustment of load was done every 15 minutes. The results of the experiments were curves over stress as a function of time. The curves have approximately the same shape, with first nearly linear increase of stress, and then curved to a maximum, and decreased, see Figure 7.

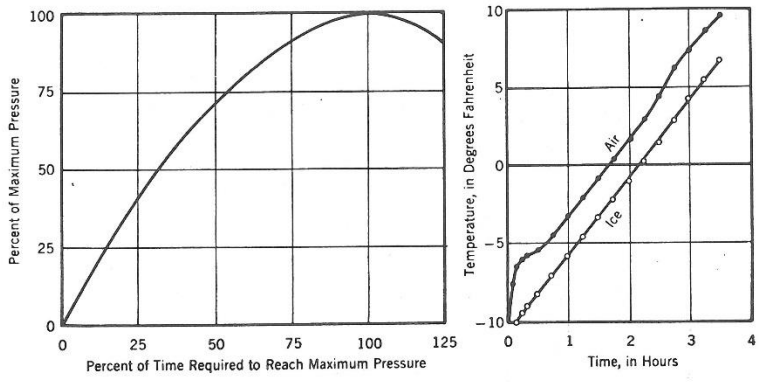

Figure 7. Average pressure-time curve (left) and air and ice temperature for typical laboratory test (right) (Monfore 1954).

The final results of experiments were summarized in two diagrams; see Figure 8, showing the maximum pressure and the time to reach the maximum as functions of the rate of change of ice temperature for different initial temperatures.

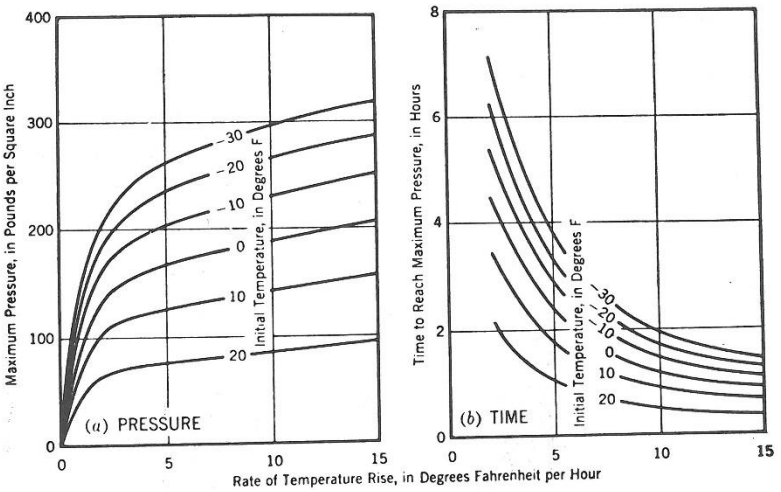

Figure 8. Maximum ice pressure (left) and time of temperature rise (right) related to the temperature rise (Monfore 1954).

Bergdahl (1978) concluded that the weaknesses of Monfore's methods are:

- uniaxial tests are used for biaxially restricted ice and that the crystal structure was not considered as a parameter.
- the phase lag of temperature (or stress) at different levels are not included in the methods.

2.5. Löfquist (1954)

Löfquist (1954) introduced a new concept for studying thermal ice pressure. The experiment was of the same type as used later by Drouin and Michel (1971) and Bergdahl (1978). Löfquist reproduced a part of an ice cover

in a cylindrical concrete basin diameter 50 cm with an insulated wall. In this container the ice was left to develop in the same way as it happens in nature by cooling the water-ice at the top surface. When the ice had reached a thickness at about 60 cm the temperature of the room was raised, the temperature of the ice surface was rising approximately from -30°C to 0°C during 15 hours.

The course of the temperature in the ice is shown in Figure 9a as given by Löfquist. The measured pressures profiles at 10, 14, and 17 hours are shown in Figure 9b. As the temperature increase penetrated through the ice, the stress profile developed into the shape of a half pear with a maximum moving down through the ice some hours delayed with respect to the minimum of the temperature curve. The maximum total ice pressure was measured to 20 t/m about 14 hours after the start of the temperature increase.

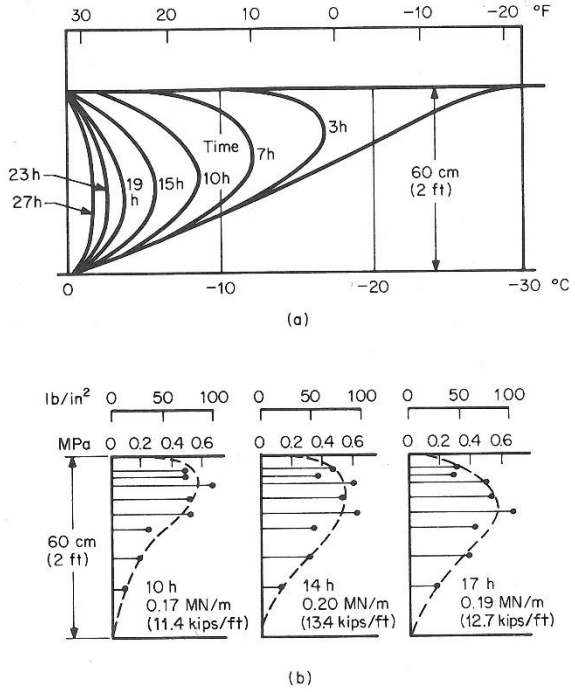

Figure 9. Results presented by Löfquist (1954): measured ice temperature (a) and pressures (b) in the ice sheet.

The cylindrical container used by Löfquist (1954) was made of concrete. Because of that, it was assumed that the thermal and elastic expansions of the concrete and some cracks in the cover during heating had caused the measured stresses to be less that it ought to be.

2.6. Assur (1959)

Assur used a quasi-linear model for the rheology with a temperature and stress dependent creep law, solved the equation for constant rate of change of temperature, and finally, formulated a differential equation for the elastic buckling of the ice cover when not loaded symmetrically.

In Assur's model, the creep deformation of ice under a load was approximately described by a rheological model with a Maxwell and a Kelvin-Voigt units in series, see Figure 10.

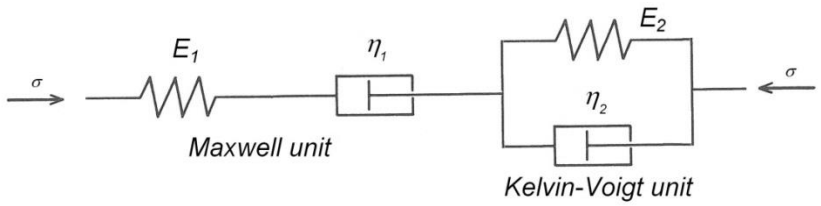

Figure 10. Rheological model with Maxwell and Kelvin-Voigt units in series.

A solution for constant load presented by Assur is:

$$\varepsilon = \frac{\sigma}{E_1} + \frac{\sigma}{m\ S}\left[\frac{t_0}{\eta_2}\left(1 - e^{-t/t_0}\right) + \frac{t}{\eta_1}\right] \tag{12}$$

where σ is compressive stress; t is time from the load application; $t_0 = E_2 / \eta_2$ is relaxation time for elastic lag; E_1 and E_2 are elastic moduli; η_1 and η_2 are viscosity moduli; m is a factor depending on the load case; S is a function of temperature and stress and 1 and 2 indices for the Maxwell and Kelvin-Voigt units, respectively.

For the uniaxial case $m = 2(1+\nu)$, and for the biaxial case $m = 2/\nu$, where $\nu = 0.5$ for the case of viscous flow:

$$S = \exp(Q_C / RT)\frac{\tau / \tau_0}{\sinh\ \tau / \tau_0} \tag{13}$$

where Q_S is the activation energy for creep; R is the universal gas constant; T is the absolute temperature; $\tau = \sigma / m$; $\tau_{-0} = cT$ and c is a constant.

Neglecting the elastic lag (the first term within the brackets in Eq. (12)), the differential equation was given as:

$$\dot{\sigma} + \frac{E_1 \sigma}{m \eta_0 S} = \alpha E_1 \dot{T} \tag{14}$$

which actually is similar expression as Eq. (31) (the rheological model by Bergdahl) for the rate of deformation:

$$\dot{\varepsilon} = \alpha \dot{T} \tag{15}$$

The maximum ice pressure $\sigma_{\max}$ was calculated from Eq. (14) for $\dot{\sigma} = 0$ as:

$$\sigma_{\max} = \alpha \ m \ \eta_0 \exp(Q_C / RT) S_1 \dot{T} \quad (16)$$

where α is the linear coefficient of thermal expansion; $\dot{T}$ is the rate of warming and S_1 is unit for low stresses which can be calculated as:

$$S_1 = (\sigma_{\max} / mcT)\sinh(\sigma_{\max} / mcT) \quad (17)$$

Assur gave values equivalent to $\eta = 0.4172 \cdot 10^{-10} tonnes \cdot h / m^2$; $Q_c = 81 \ kJ / mol$; $R = 8.31 \ J / (mol \cdot K)$; $c = 0.154 \ tonnes / (m^2 K)$; $\alpha = 51.5 \cdot 10^6 \ °C^{-1}$; $E_1 = 0.65 \cdot 10^6 tonnes / m^2$.

Assur also gave a non-dimensional solution of the complete function for a constant rate of change of temperature by searching unknown functions:

$$\sigma_{\max} = -aT_0(1 - bT_0)\left(\dot{T} + \dot{T}_1\right) \quad (18)$$

where T_0 is the initial temperature; a, b and $\dot{T}_1$ are constants: with $a = 0.33964 \ tonnes/(m^2 °C)$; $b = 0.010137 \ °C^{-1}$ and $\dot{T} = 21.1 °C/h$.

The agreement with test results given by Monfore was said to be excellent with a correlation coefficient of 0.9986 for $\dot{T} \geq 2.5 \ °C/hour$. Assur pointed out that the total lateral force to a considerable degree depends on the depth of penetration of the warming wave and is limited by the buckling, if the ice cover is thin. He criticized the use of the assumption of an axial load at half the depth of the ice cover, and he proposed a corrected equation probably based on an assumed unfavourable stress distribution (Bergdahl 1978).

2.7. Lindgren (1968)

The work presented by Lindgren (1968) contained laboratory tests with both uniaxial and biaxial load. The results of the experiments were utilized in a method to calculate the thermal ice pressure in an ice cover for a prescribed air-temperature variation.

The uniaxial tests were performed with ice prism that were loaded with constant weights at - 10°C equivalent to 2, 6, 8, 10 and 14 pk/cm^2 [1], and at -0.5°C, - 5°C and - 20°C equivalent to 6 pk/cm^2. The deformation as a function of time was measured during these investigations. Biaxial experiments with restricted thermal expansion were also made with circular ice plates that were placed in a steel ring, where the small space

[1] [pk/cm^2] – [kilolibra/cm^2]. $1 pk/cm^2 * 0.0981 = 0.981 MPa$

between the ice and ring was filled by water. Tests started at low temperatures after which the temperature was raised. The temperature, the strain and the stress were recorded as a function of time.

To present the results of the laboratory tests in a common form, Lindgren tried to fit the parameters in a linear viscoelastic model composed of a Maxwell and a Kelvin-Voigt element couplet in series.

The rheological equation for such model is:

$$\varepsilon = \frac{\sigma}{E_1} + \frac{\sigma}{E_2}\left(1 - \exp\left(-\frac{E_2 t}{\eta_2}\right)\right) + \frac{\sigma\, t}{\eta_1} \tag{19}$$

where E_1 and E_2 are elastic moduli; η_1 and η_2 are viscosity moduli; ε is strain; σ is stress; 1 is index for the Maxwell unit and 2 is index for the Kelvin-Voigt unit.

Lindgren gave the following values from uniaxial experiment:

$$E_1 = 66000\left(1 - 0.012\Theta\right) \ (kp/cm^2)$$

$$E_2 = 70000 \ (kp/cm^2)$$

$$\eta_1 = 18.5 \ \sigma^{-1}\left(0.20 - 0.08\Theta\right)\left(\frac{t}{3600}\right)^{0.5} \cdot 10^8 \ (kp \ \sec/cm^2) \tag{20}$$

$$\eta_2 = 1.1 \cdot 10^8 \ (kp \ \sec/cm^2)$$

From the biaxial test Lindgren estimated the same values of and as for the uniaxial test with the assumption that Poisson's modulus was 0.36. The values of η_2 was assumed to be the same while a new equation was used for η_1 (in $kp \ \sec/cm^2$):

$$\eta_1 = 31 \ \sigma^{-1}\left(0.30 - 0.07\Theta\right)\left(\frac{t}{3600}\right)^{0.25} \cdot 10^8 \tag{21}$$

on condition that Poisson's ratio 0.5 was for the viscous deformation.

In the thermal analysis Lindgren established that the influence of the growing of the ice cover on the thermal gradient can be disregarded. For calculation of the temperature profile in the ice for arbitrarily changes of air temperature a graphical variant of Schmidt difference scheme was used in Lundgren model.

2.8. Jumppanen (1973)

The thermal ice pressure was studied by Jumppanen (1973). Cylindrical specimens were loaded axially at stress level 3, 7 and 12 kp/cm^2 at temperatures of -2°C, -5°C, -12°C and -25 °C. The specimens were cut with their axes horizontal and parallel to c-axes of grains, and were taken from artificial ice covers produced from tap water and from an ice cover in the Saima Canal in Finland.

Jumppanen analysed his data using a viscoelastic model similar to Lindgren's. For a linear material the creep compliance $J(t)$ is a monotonously increasing function for $t \geq 0$, and for $t < 0$ $J(t) \equiv 0$. For a constant stress σ_0 applied to a material obeying the same differential equation as the one used by Lindgren (1968), the deformation ε as a function of time t can be written:

$$\varepsilon = \sigma_0 J(t) = \sigma_0 \left[\frac{1}{E_1} + \frac{1}{E_2}\left(1 - e^{-t/t_0}\right) + \frac{t}{\eta_1} \right] \tag{22}$$

The compliance function proposed by Jumppanen based on several uniaxial loading tests on cylindrical specimens is:

$$J(t) = a + bt^n \tag{23}$$

where $n = 0.3$, t is time in hours; and a and b are linearly dependent on temperature as:

$$a(\Delta T) = (1.17 + 0.036\Delta T)\cdot 10^{-5} \ \ cm^2 / kp$$
$$b(\Delta T) = (24.5 + 0.5\Delta T)\cdot 10^{-5} \ \ cm^2 / kp \text{ for artificial ice}$$
$$b(\Delta T) = (12 + 0.25\Delta T)\cdot 10^{-5} \ \ cm^2 / kp \text{ for Saima Canal ice} \tag{24}$$

with

$$\Delta T = T + 25°\mathrm{C} \quad \text{for } -25°\mathrm{C} \leq T \leq 0°\mathrm{C}$$

The value of $b(\Delta T)$ was quite different for artificial ice and the Saima Canal ice. According to Jumppanen this was probably caused by the air content of the artificial ice, and by the fact the canal ice had earlier been loaded by temperature changes of the ice cover. The compliance function was finally used for calculation of the expansion of a circular ice plate, a square ice plate and an ice plate in a long trough. The solution did not involve the calculation of temperatures in the ice cover. Comparison of the measured and calculated values is presented in Figure 11.

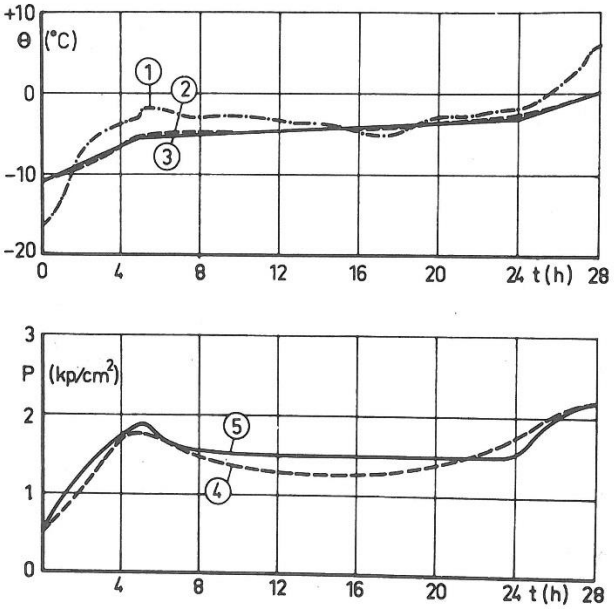

Figure 11. Values of ice pressure at the Saima Canal. 1) Air temperatures; 2) Ice temperatures at the depth 8 cm; 3) Approximated ice temperature for the calculations; 4) Measured ice pressure at the same depth; 5) Calculated ice pressure (Jumppanen 1973).

2.9. Drouin and Michel (1971, 1974)

Drouin and Michel (1971) presented an extensive investigation of the thermal ice pressure. The study of uniaxial deformation of ice and biaxially restricted expansion tests of the same type as made by Lindgren (1968) with better controlled conditions.

In uniaxial test cylindrical samples with length of 76.2 mm and diameter of 25.4 mm, were deformed along the axis at a constant strain rate and a constant temperature. The loading direction was always parallel to the surface of the ice. Three types of ice were tested:

Manufactured snow ice with porosity about 3.3% and reported density 810 kg/m^3. The diameter of grains was about 1 mm and the direction of the crystallographic orientations was random (38 tests).

Manufactured columnar ice of the type S1, where the c-axes of the crystals are vertical or nearly vertical. The stress was perpendicular to the c-axes (26 tests).

Manufactured columnar ice of the type S2, where the c-axes is horizontal. The average gain size measured perpendicular to the long direction of the grains was about 2 mm (2 tests).

After some tests had been made, Drouin and Michel concluded that the samples of the S2 ice were too small compared to the grain size. Only two tests with bigger samples are then reported with dimensions of height of 101.6 mm and diameter of 50.8 mm.

Brouin and Michel used the dislocation theory to improve constant-strain-rate curves. The rheological model of Drouin and Michel is of the following form:

$$\frac{d\sigma}{dt} = \dot{\varepsilon} E_a - 2b\beta E_a \left(\left(\frac{n_0}{\beta} + \dot{\varepsilon} t \right) - \frac{\sigma(t)}{E_a} \right) \left(\frac{\sigma(t)}{2p} \right)^m \tag{25}$$

where σ is stress; $\dot{\varepsilon}$ is strain rate; t is time; E_a is apparent elastic modulus; n_0 is initial number of dislocations; β is rate of multiplication of dislocations; b is the Burger vector and p and m are constants.

The necessary material constants (a total of six: E_a, n_0, β, b, p, m) were obtained partly as fitting constants to the experiments. The surface temperature of the ice cover is assumed to be equal to the air temperature. The ice temperature is initially assumed to increase linearly from the surface to the ice-water interface, where it is 0 °C. If the air temperature is subjected to fluctuation:

$$T_a = \frac{T_0}{2} + \frac{T_0}{2} \cos \frac{2\pi t}{t_0}, \; 0 < t < \frac{t_0}{2} \tag{26}$$

where T_0 is the initial air temperature and t_0 the period of the cycle.

The variation of the temperature in the ice cover more than 40 cm thick due to a cyclic temperature variation at the surface was approximated by the Fourier-solution for a semi-infinite space. At any depth z of the cover it is given by:

$$T(z,t) = \frac{T_0}{2} \left[1 + \exp\left(-z \sqrt{\frac{\omega}{2d}} \right) \cos\left(\omega t - z \sqrt{\frac{\omega}{2d}} \right) \right] \tag{27}$$

where $\omega = \frac{2\pi}{t_0}$ and d is the thermal diffusivity of ice, assumed to be $1.16 \cdot 10^{-6}$ m^2/s.

However, Bergdahl (1978) showed that the calculation of the temperature distribution may not be correct.

Differentiating the equation with respect to time gives:

$$\frac{\partial T}{\partial t} = \dot{T}(z,t) = -\frac{\pi T_0}{t_0} \left[\exp\left(-z \sqrt{\frac{\omega}{2d}} \right) \sin\left(\omega t - z \sqrt{\frac{\omega}{2d}} \right) \right] \tag{28}$$

On the other hand, strain is related to temperature change by:

$$\dot{\varepsilon} = \alpha \dot{T} \tag{29}$$

The coefficient of thermal expansion of ice decrease slightly with decreasing temperature and is expressed in the form:

$$\alpha = (5.4 + 0.018T) \cdot 10^{-5} \ ^{\circ}\mathrm{C}^{-1} \tag{30}$$

When the strain rates at different levels of the ice cover and the rheological model for ice are known, the thermal pressure can be computed numerically step by step.

Based on the tests graphs have been computed which show the maximum total thermal ice pressure that is exerted by an ice cover (composed of S1 ice and uniaxially restrained) as a function of cover thickness and with initial surface temperature of the ice and the time for increasing this temperature from 0 °C (half period of the sinusoidal variation as parameters).

2.10.Metge (1976)

Metge (1976) (from Ashton 1986) presented the basic assumptions about cracks in the ice and drew some important conclusion which should be incorporated into the methods for calculating thermal ice pressure. The basic assumptions in most methods are that the tension is completely released when the crack is formed, that all cracks become filled by water, and that this water is completely frozen when the ice starts to expand again. Thermal cracks fall into three groups characterized by different behaviour: dry cracks, narrow, wet cracks; and wide cracks.

Dry cracks: Dry cracks form as following: during a cold night, the top of the ice cools, while bottom remain at 0°C. This cause that ice becomes concave, until the moment due to the weight of the edges is so large that the sheet cracks. This process is repeated until each piece of uncracked ice is small enough to withstand the curvature. The cracks do not usually fill with water because the cracking does not result in separation of the pieces. Dry cracks act as bellows, opening and closing according to ice temperature. These cracks are always present in a cold ice cover, where they absorb a significant part of the thermal ice movement, reducing the potential thermal ice pressure significantly.

Figure 12 shows a typical section of a dry crack. The crack is straight down to about 2/3 of the ice thickness, where t is met by one or two shear cracks, usually at 45° to the vertical. Although these shear cracks are easily visible because of reflected light, they are not open and do not let any water though.

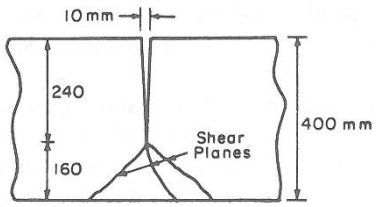

Figure 12. Section of a dry crack (Metge 1976).

Narrow, wet cracks: These cracks are narrow enough to refreeze rapidly and in doing so add material to ice sheet. The existence of this process was proven from thin section of these cracks, which show the layer of new ice added, see Figure 13. When the sides of a dry crack separate, the water rises to approximately 90 % of the ice thickness, with some adjustment for the deflection of the ice sheet due to thermal stresses or snow load.

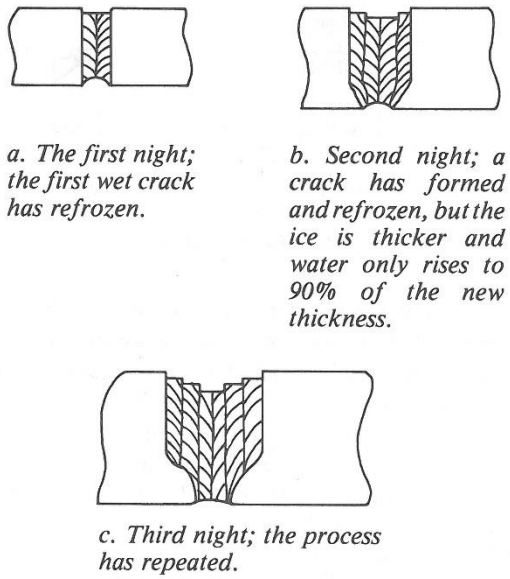

Figure 13. Repeated addition of ice to a narrow wet crack (Metge 1976).

Wide cracks: The overall contraction of an ice sheet is mostly concentrated at one or two cracks, which usually form near tensile rises, such as between two headlands. In a long channel, wide cracks form a fairly regular interval across the channel, while other cracks skirt the shore form headland to headland. Some cracks are more than 20 cm wide. The large volume of water in these cracks cannot freeze completely during one night, so by morning a typical wide crack has taken the shape shown in Figure 14a. If the ice temperature rises the next day, the thin bridge of ice across the crack is put in compression and will suddenly fail. The crack may close, producing a noise and violent impact. The ice bridge usually fails in shear along an inclined plane, and one side of the crack slip over the other (Figure 14b). In this way a pressure ridge has started to form. Another mechanism is caused by the fact that the bridge is formed near the top of the ice sheet. During compression a moment applied to the sheet, and if it is thin, the sheet may fail in bending. If a cold period lasts for weeks, even wide cracks will refreeze to a considerable extent and will be sufficiently strong to sustain the eventually thermal expansion.

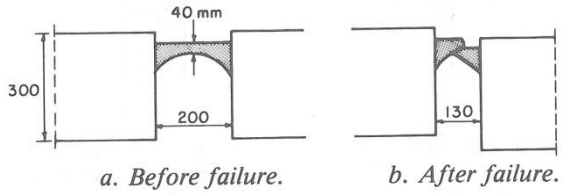

Figure 14. Typical wide crack (Ashton 1986).

The main conclusion is that in a wide crack a pressure ridge may be initiated at compressive stresses associated with the crushing strength of the ice or the buckling load of the ice cover. For thermal pressure this is limited by the strength of the bridge, and the resulting impact load can become as much as three times the failure load of the bridge.

2.11.Bergdahl (1978)

Some of investigators acknowledged that linear viscous-elastic models give an unsatisfactory description of the stress-strain relationship of ice (Ashton 1986). Bergdahl (1978) proposed a simple nonlinear rheological model composed of a linear spring in series a nonlinear dashpot, see Figure 15.

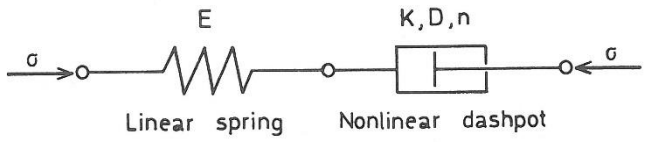

Figure 15. Nonlinear rheological model used by Bergdahl (1978).

The differential equation of the model is:

$$\dot{\varepsilon} = \frac{\dot{\sigma}}{E} + KD(\sigma)^n \tag{31}$$

where K and n are functions of strain rate, and E and D are functions of temperature.

The modulus of elasticity E (MPa) was based on the results by Lindgren (1968) and Gold (1958) and was expressed as:

$$E = 6.1(1 - c \cdot T) \tag{32}$$

where $c = 0.012\,°C^{-1}$ and T is the ice temperature, °C.

The temperature dependence of the viscous creep rate was described by the Arrhenius equation for diffusion:

$$D = D_0 \exp\left(-Q_s / RT_{abs}\right) \tag{33}$$

where $D_0 = (9.13 \pm 0.57) \cdot 10^{-4}\ \ m^2/s$; $Q_s = 59.8\ \ kJ/mole$, the activation energy; $R = 8.31\ \ J/mole \cdot K$ (the gas constant) and T_{abs} is absolute temperature, K.

The basis for the values of K and n is the experiments by Drouin and Michel (1971) on ice monocrystals loaded parallel to the basal planes. The constant strain rate tests have been evaluated for the maximum stress when $\dot{\sigma} = 0$ of the differential equation of the model. The results was $K = 4.40 \cdot 10^{-16}$ (m $^{-2}$ Pa $^{-n}$) and $n = 3.651$ for the temperature compensated rate range:

$$2 \cdot 10^7 < \dot{\varepsilon}/D < 8 \cdot 10^9\ (m^{-2}) \tag{34}$$

In Figure 16 stress as a function of a constant strain rate at $\dot{\varepsilon} = 1.45 \cdot 10^{-8}$ s $^{-1}$ calculated with Bergdahl's model and Drouin's and Michel's model is compared (Bergdahl 1978). Calculations using Bergdahl's equation yielded higher pressure than similar calculations made by Drouin and Michel. The reason was mainly the choice of modulus of elasticity $E = 6.1$ GPa compared to Drouin's and Michel's 1.5 GPa. The strain softening proposed by Drouin and Michel reduced their ice load calculations and thus Bergdahl's results appeared to be much too high (Fransson 1988).

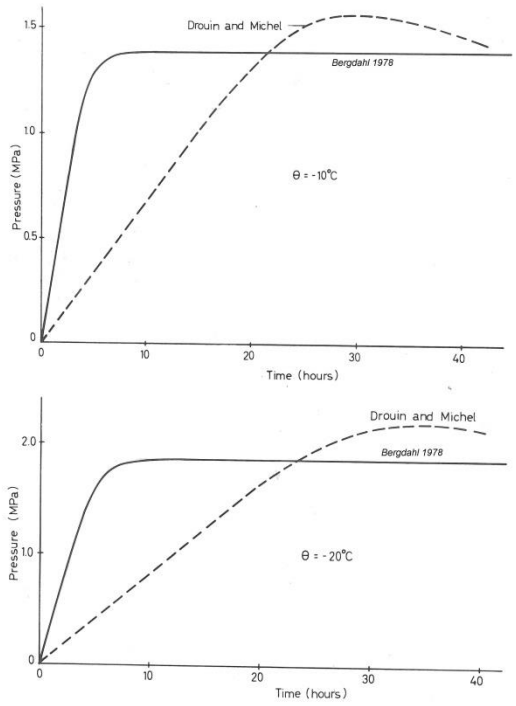

Figure 16.Stress as a function of time for constant rate of strain $\dot{\varepsilon} = 1.45 \cdot 10^{-8} s^{-1}$: a) at $-10°C$; b) $-20°C$ (Bergdahl 1978).

The calculated temperature profile can be used to calculate the thermal ice pressure for each depth interval separately. The pressures are then integrated over the depth of ice which gives the total ice pressure (N/m).

The rate of deformation is the coefficient of linear thermal expansion times the rate of change of temperature:

$$\dot{\varepsilon} = \frac{d\varepsilon}{dt} = \alpha \frac{dT}{dt} = \alpha \dot{T} \tag{35}$$

which with the differential equation of the model gives:

$$\alpha \cdot dT = d\varepsilon = \left(Ed\sigma / dt + KD\sigma^n\right)dt \tag{36}$$

This can be written on difference form as:

$$\sigma_{k+1} = \sigma_k + E_m\left[\Delta\varepsilon - \left(D_k K\sigma_k^n + D_{k+1}{\sigma_{k+1}}^n\right)\frac{\Delta t}{2}\right] \tag{37}$$

where σ_k is the stress at the point of time $t = k\Delta t$; σ_{k+1} is the stress at $t + \Delta t 0(k+1)\Delta t$; $\sigma_{k+1} - \sigma_k = \Delta\sigma$; E_m is the elasticity modulus of the ice for $T = \left(T(t) + T(t+\Delta t)\right)/2$; D_k is the self-diffusion for $T(t)$ and D_{k+1} is the self-diffusion for $T(t+\Delta t)$.

This equation can be solved for the stresses using the interactive procedure. The stresses are integrated over the depth of the ice cover, and if the integrated ice pressure is greater than an elastic buckling load, the thermal ice pressure is set to that lower value. The limiting load is set to:

$$P_b = 2\sqrt{\rho_w g E h^3 / 12(1-\nu^2)} \tag{38}$$

where ρ_w is the density of water; g is the earth acceleration; E is the elasticity modulus of ice at the mean depth of the ice cover, Eq. (32); h is the thickness of the ice cover and $\nu = 0$ is the Poisson's modulus.

The comparison between the proposed model and some others models (Royen, Jumppanen, Assur and Lindgren) was presented by Bergdahl (1978), see Figure 17.

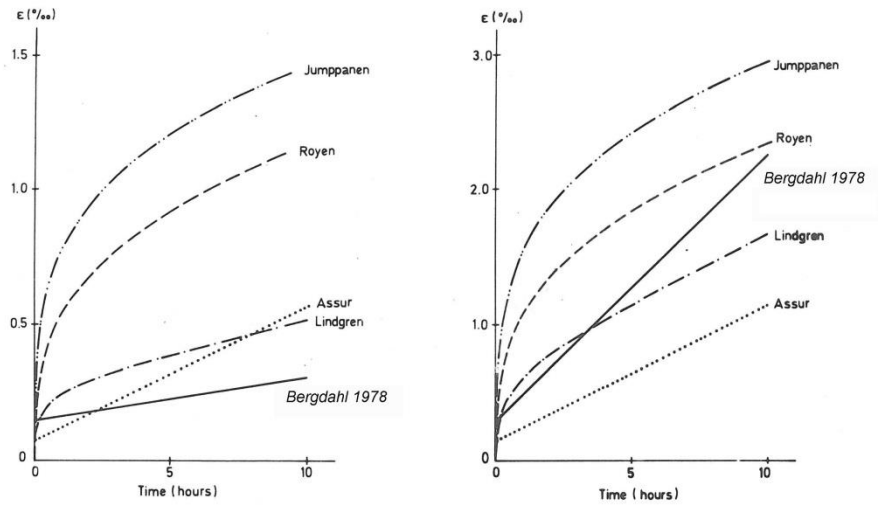

Figure 17. Deformation as a function of time for the constant stresses: a) $\sigma = 1MPa$ and b) ice temperature $-10°\mathrm{C}$ and two-axial deformation (Bergdahl 1978).

2.12.Cox (1984)

Cox (1984) reported the results of measuring the ice pressure in the cover of small lake using a biaxial stress sensor. Bergdahl's rheological model was used to calculate the ice stress during the study. As the ice was warm (never colder than -3°C at the depth of the sensing portion of the stress gauge) and presumably ductile, the model by Bergdahl was modified to allow tensile stresses to accumulated in the ice cover during cooling periods without any cracking.

As Bergdahl, a finite difference scheme was used to calculate the ice pressure. However, a Newton's method rather than successive substitution was used to solve the nonlinear equation. From Bergdahl:

$$\sigma_2 = \sigma_1 + \bar{E}\left[\Delta\varepsilon - \left(D_1 K \sigma_1^n + D_2 K \sigma_2^n\right)\frac{\Delta t}{2\sigma_*^n}\right] \tag{39}$$

and the subscripts denote the value of the parameters at times 1 and 2.

The ice thermal strain during the time step Δt is calculated from:

$$\Delta\varepsilon = \varepsilon_2 - \varepsilon_1 = \alpha\left(T_2 - T_1\right) \tag{40}$$

where α is the linear coefficient of thermal expansion and T is the ice temperature.

Applying Newton's methods to solve for σ_2 the following equation can be obtained:

$$\sigma_2(new) = \sigma_2 + \frac{\sigma_1 - \sigma_2 + \bar{E}\left[\Delta\varepsilon - \left(D_1 K \sigma_1^n + D_2 K \sigma_2^n\right)\frac{\Delta t}{2\sigma_*^n}\right]}{1 + n\bar{E} D_2 K \sigma_2^{n-1}\frac{\Delta t}{2\sigma_*^n}} \tag{41}$$

The computed stress-time history using Bergdahl's model and recommended values for E, K, D and n was compared to the measured stress, see Figure 18. In general, it was concluded by Cox that Bergdahl's model over-predicts compressive and tensile stresses in the ice.

The conservative (high) values of maximum stress were explained partially by Bergdahl's selection of E, K and D. Cox used a lower effective modulus $E = 4$ GPa of ice to describe the elastic behaviour of the ice while Bergdahl recommended the values of 6 GPa.

Additionally, Bergdahl used the Arrhenius equation to describe the effect of temperature on the creep rate of ice. Cox defined a new function based on the experimental work by Drouin and Michel (1971) which showed a very strong temperature dependence of creep rate of S1 ice such that

$$\dot{\varepsilon} = \frac{\dot{\sigma}}{E} + A(T)\left(\frac{\sigma}{\sigma_*}\right)^n \tag{42}$$

where in a constant strain-rate test:

$$A(T) = \frac{\dot{\varepsilon}}{(\sigma_{\max}/\sigma_*)^n} \tag{43}$$

or, in a constant load test:

$$A(T) = \frac{\dot{\varepsilon}_{\min}}{(\sigma/\sigma_*)^n} \tag{44}$$

From the curves presented by Droiun and Michel values of $\sigma_{\max}$ where obtained for a strain-rate of 2×10^{-8} s^{-1}. Then the values of $\ln A(T)$ were plotted against the values of $\ln(T)$. To provide a linear fit of the data, it was assumed that the 0°C tests were performed at -1°C. By adjusting the data:

$$A(T) = B\left(\frac{T}{T_*}\right)^m \tag{45}$$

where $B = 2.46\cdot10^{-29}$ s^{-1}; $m = 1.92$; $T_* = -1$°C (unit of temperature) and T is the ice temperature, °C.

According to Fransson (1988) Eq. (45) presented by Cox (1984) must contain a typing error and should be:

$$A(T) = B\left(\frac{T_*}{T}\right)^m \tag{46}$$

By using E and $A(T)$ the new values of the thermal stresses were calculated and compared to measured values and values obtained by the Bergdahl model. Better agreement was obtained between the measured and calculated values using the Cox's modification of the Bergdahl model (Figure 18).

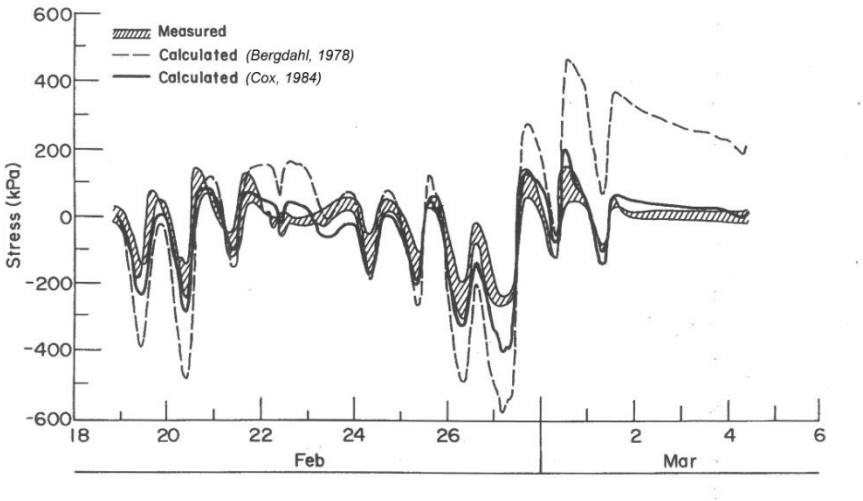

Figure 18. Calculated and measured values obtained by the Bergdahl model and the Cox's modification (Cox 1984).

2.13.Xu Bomeng (1981, 1986)

Xu, based on the data collected from reservoirs in Northern China presents an empirical formula to predict the average pressure of ice sheet:

$$P = K \cdot K_s \cdot C_h (3 - t_a)^{1/2} \Delta t_a{}^{1/3} \left(T^{0.26} - 0.6\right) / - t_a{}^{3/4} \tag{47}$$

where P is average pressure of ice sheet, kg/cm^2 ; t_a is initial air temperature at 8 a.m., °C (usually not exceeding -10 °C); Δt_a is increment in air temperature rising (°C) from 8 a.m. to 2 p.m., or from 8 a.m. of the first day to 2 p.m. of the second or third day for sustained temperature rising; the highest air temperature should not exceed 0°C; T is duration of sustained temperature rising (hours) corresponding to Δt_a - for ordinary weather $T = 6$ hours, for successive days of air temperature rising $T = 30$ hours (two days); K_s is factor of snow cover, in case of no snow $K_s = 1.0$; C_h is conversion factor related to thickness of ice which is equal to 0.391, 0.311, 0.274, 0.252 and 0.237 corresponding to the ice thicknesses of 40, 60, 80, 100 and 120 cm, respectively; K is coefficient to account for the overall effect of others factors.

The design value of the ice pressure expressed in total ice pressure in one unit of length can be obtained as the following relationship:

$$P = 13.73h \cdot K \cdot C_h \cdot m_t \tag{48}$$

where P is design ice pressure (t/m); h is ice thickness (m) and m_t is time factor of temperature rise (1.0 or 1.82).

The ice pressure values computed with Eq. (48) are presented in Figure 19.

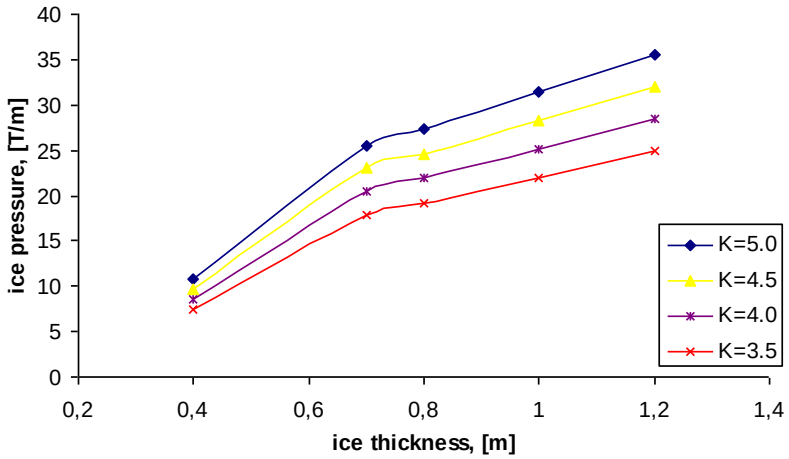

Figure 19. Relationship of ice pressure and ice thickness (Xu 1986).

2.14.Fransson (1988)

Two steps process for determination of the ice pressure were suggested by Fransson (1988): simple analytical determination of the maximum ice pressure at the centre of ice and calculation of the maximum load by assuming a pressure distribution through the ice. A possible approximation of the sum of the pressure in an ice cover can be based on the stress development in the centre of ice. Therefore a link between the air temperature history and the resulting temperatures in the centre of the ice was suggested by Fransson.

The temperature at any depth x and time t in the ice cover can be calculated assuming one-dimensional heat conductivity. Solar radiation and other heat sources were neglected during the time of the year when maximum ice thrust is expected. The temperature rise at the centre of the ice is approximated to a straight line with the coefficient $b_{0.5}$ during the period of time when the total ice pressure increases. The relation between the linearized function used by Fransson and the original temperature function, see Figure 20.

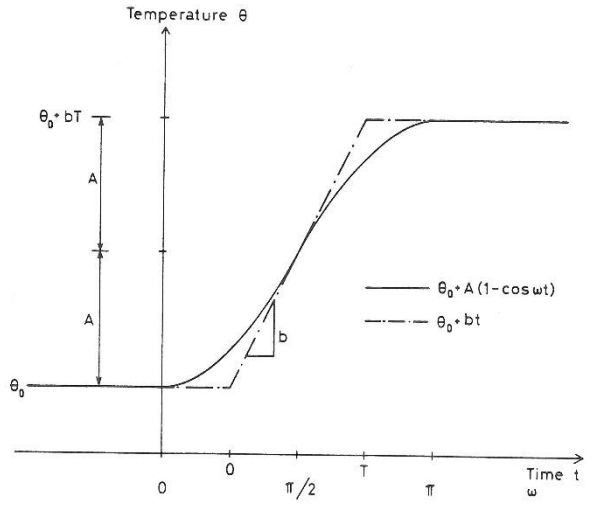

Figure 20. Relationship between the used linearized function and the original temperature function (Fransson 1988).

The rheological model used by Fransson consists of a linear spring in series with a nonlinear and temperature dependent dashpot. The stress σ corresponds to uniaxial stress. The rheological equation is:

$$\dot{\varepsilon} = \frac{1}{E}\dot{\sigma} + B\left(\frac{\sigma}{\sigma_*}\right)^n \tag{49}$$

where $\dot{\varepsilon}$ is strain rate; $\dot{\sigma}$ is stress rate; σ is stress level; σ_* is index stress; n is empirical constant; E is Young's modulus for columnar ice and B is temperature dependent strain rate.

The temperature dependence of the creep rate can be expressed as:

$$B = B_0\left(\frac{T_*}{T_1 - T}\right)^m \tag{50}$$

where T is temperature; T_* is index temperature ($+1°\mathrm{C}$); T_1 and m are empirical constants and B_0 is strain rate at $T = 0°\mathrm{C}$ and $\sigma = \sigma_*$.

The proposed rheological model by Fransson for S1 ice is basically the same as the model by Bergdahl and Cox. However, one difference is that n is an empirical constant adjusted to field data. Young's modulus for S1 ice can be obtained from accurate measurements on single crystals, eventually with some reduction because of air content and microcracks.

By definition of thermal stress with complete restraint, follows that the expansion strain rate is equal to the deformation strain rate, such that:

$$\dot{\varepsilon} = \alpha \dot{T} = \frac{1}{E}\dot{\sigma} + B\left(\frac{\sigma}{\sigma_*}\right)^n \tag{51}$$

or the stress rate:

$$\dot{\sigma} = E\left[\alpha \dot{T} - B\left(\frac{\sigma}{\sigma_*}\right)^n\right] \tag{52}$$

The maximum stress is obtained for $\dot{\sigma} = 0$ is:

$$\sigma_{\max} = \sigma_*\left(\frac{\alpha \dot{T}}{B}\right)^{1/n} \tag{53}$$

where B is the creep rate at the temperature when $\sigma = \sigma_{\max}$.

The differential equation of order n can be solved numerically using a finite difference scheme. However, the lack of an analytical solution of the nonlinear rheological equation is one obstacle that has to be overcome with help of the computer calculations. Another obstacle is that the constant n cannot be obtained from simple material tests on the actual ice type passing the transient creep. That takes a very long time to do at low stress levels. In this situation it was suggested by Fransson to use an approximate stress model.

Royen's empirical equation can be expressed in a more general way, with nonlinear dependence of the temperature:

$$\varepsilon = \frac{c\sigma\, t^q}{(T_1 - T)^m} \tag{54}$$

where c, q, T_1, and m are constants.

After differentiation of ε with respect to t, the stress rate becomes:

$$\dot{\sigma} + \left(\frac{q}{t} + \frac{m\dot{T}}{T_1 - T}\right)\sigma = \frac{\dot{T}\alpha}{c}\frac{(T_1 - T)^m}{t^q} \tag{55}$$

Eq. (55) is a linear differential equation of first order which can be solved analytically as:

$$\sigma = \frac{(T_1 - T)^m}{t^q}\frac{\alpha}{c}(T - T_0) \tag{56}$$

and for linear temperature rise the maximum stress can be presented as:

$$\sigma_{\max} = f(q,m)\frac{\alpha}{c}(T_1 - T_0)^{1-q+m} b^q \tag{57}$$

where

$$f(q,m) = \left(\frac{m}{1-q+m}\right)^m \left(\frac{1-q}{1-q+m}\right)^{1-q} \tag{58}$$

Θ_1, q, m and c are empirical constants; α is linear coefficient of thermal expansion; T_0 and b are input temperature variables.

For biaxial stress field the Eq. (52) may be reformulated as:

$$\dot{\sigma} = \frac{E}{(1-\beta\ \nu)}\left[\alpha\dot{T} - \lambda B\left(\frac{\sigma}{\sigma_*}\right)^n\right] \tag{59}$$

where ν is Poisson's ratio; β is ratio between two principal stresses and λ is a factor defined as:

$$\lambda = B_0 / B_0(\beta = 0) \tag{60}$$

where $B_0(\beta = 0)$ is the creep rate at 0 °C determined from a uniaxial loading test parallel to the surface of the ice sheet.

Further, Fransson presented how potential of the thermal ice load can be assembled using an analytical solution. An ice sheet with known parameters (a, α / c) and with a complete lateral restraint. The boundary conditions at the upper surface are given by the temperature history shown in Figure 21.

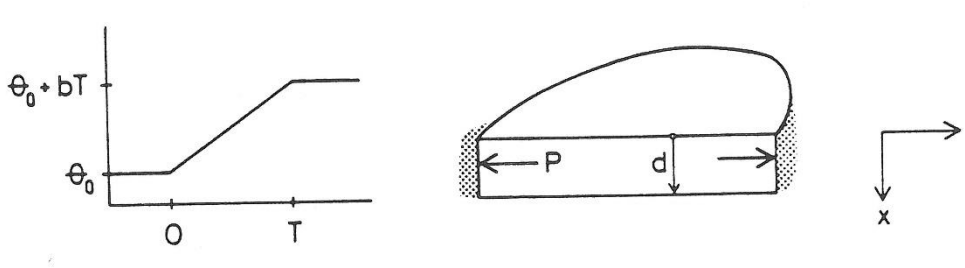

Figure 21. Analytical temperature rise on the surface of an ice sheet with complete lateral restraint (Fransson 1988).

An analytical expression of the potential of ice pressure in the ice centre was written as:

$$\sigma_{0.5}^{\max} = a_1(-T_0)b^{0.5}\exp\left[-a_2\ d(-b/T_0)^{0.5}\right] \quad \text{for } 0.2 < d < 2m \tag{61}$$

$$\sigma_{0.5}^{\max} = a_3(-T_0)^{1.5}d^{-1} \qquad \text{for } d > 0.5m \tag{62}$$

where $a_1 = 0.224(\alpha/c)$; $a_2 = 2.49$ and $a_3 = 0.331(\alpha/c)$.

The total horizontal force P from the ice pressure can be estimated as:

$$P = \beta\ \sigma_{o.5}^{\max} d \tag{63}$$

where β is a function of the shape of the stress distribution ($\beta = 1$ if rectangular).

Based on the experimental study by Löfquist (1954), the value $\beta = 0.7$ was used by Fransson. The pressure distribution is presented in Figure 22.

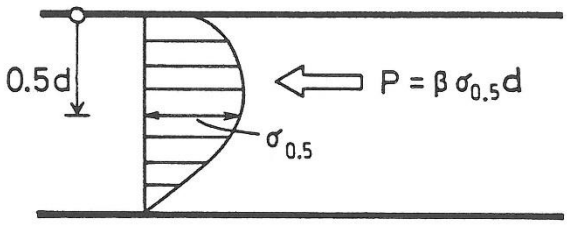

Figure 22. Assumed relationship between maximum pressure and the resulting maximum force (Fransson 1988).

The reduction because of closure of dry cracks at the ice surface can be included using the proposed values of ΔT:

$$\begin{cases} \Delta T = 5L / L_C & 0 \le L \le L_C \\ \Delta T = 5°\mathrm{C} & L > L_C \end{cases} \tag{64}$$

where L is the total length of the confined ice sheet; $L_C = 100d$, the distance between two major thermal contraction cracks and d is the ice thickness.

Also reduction because of incomplete restraint or large, wide cracks can be considered applying the following relation:

$$P_C / P = (1-\gamma)^{1+(1/n)} \tag{65}$$

where P_C / P is the reduction of the potential of ice thrust; γ is the crack depth and n is the empirical stress exponent; $n = 2$.

The reduced load P_C can be expressed as:

$$P_C = P(1-\gamma)^{1.5} \tag{66}$$

A practical formulation of the potential of thermal ice load P_c can be assembled using Eqs. (56), (57) and (60):

$$P_C = \beta\ a_3[(1-\gamma)(-T_0 + \Delta T)]^{1.5} \tag{67}$$

where $a_3 = 0.0331\ \alpha / c$ and T_0 is the initial ice surface temperature.

In most situations very limited information is available for the actual ice conditions at the location of the structure. Based on the presented work by Fransson (1988) a simple design formula that may serve as guidance for engineers can be established:

$$P_C = 2\left(-T_0\right)^{1.5} \tag{68}$$

where T_0 is the initial temperature (°C).

The temperature should be chosen as the coldest week- temperature during a 10-year period according to the closest weather station. At the areas where the ice thickness is less that 0.5 m the thermal ice load may be lower than predicted by presented formula (Fransson 1988).

2.15.Carter et al. (1998)

Carter et al. (1998) undertook a 3-year program from 1995 to 1998 to measure the static ice forces in four reservoirs in central and northern Quebec. In this program, changes in measured stress in an ice sheet have been correlated with changes in air temperature; it may arise from water level variations, wind and current drag force. Measurements indicated that the ice pressure changes with increasing water level; the maximum values were about 150 kN/m.The field investigations revealed two facts that ice cover have circumferential cracks caused either by water level variation or thermal contraction, and the static ice forces are, in some instances, sufficient to trigger an instability of the broken ice covers by buckling.

To investigate stability of ice floes, a two-dimensional analysis was considered by Carter et al. (1998), in which wide ice floes are pushed by in-plane force against a dam wall, see Figure 23. Previously, Kovacs and Sodhi (1980) have discussed the stability of two ice floes by considering the potential energy of the system arising from buoyancy effects and elastic hinges at the end of the floes. As rotation of ice floes usually results in permanent damage to ice at the end of a floe, it was suggested by Sodhi (1995, 1998) to consider plastic, instead of elastic, hinges at the ends of the floes. Assuming a velocity field for the system shown in Figure 23, Sodhi and Carter (1998) have used plastic limit analysis to determine the force per unit width of ice sheet required to cause instability.

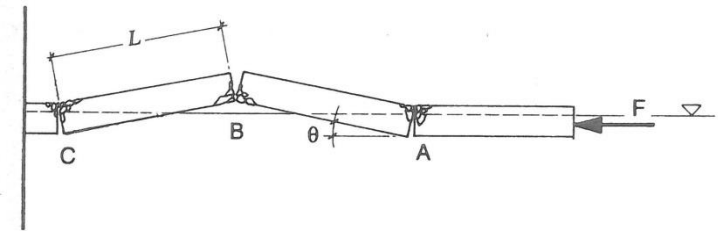

Figure 23. Model for in-plane compressive force displacement of ice floes (Carter et al. (1998).

For an assumed velocity field of the system, see Figure 23 , point A moves horizontally at a velocity of *2V* , and point C does not move. Point B moves horizontally at a velocity of *V* and vertically at a velocity of $V \cot \theta$,

where θ is the angular position of the floe. The velocity of other points on floes AB and BC is linearly proportional to the velocity at the ends of a floe. Considering a unit width of an ice sheet, the rate of change of potential energy E_b, arising from buoyancy effect is than obtained as:

$$\frac{dE_b}{dt} = \frac{2}{3}\rho g L^2 V \cos\theta \tag{69}$$

where ρg is the specific weight of water and *L* is the floe length.

With respect to adjacent ice sheets, the rate of rotation of these floes at points A and C is:

$$\frac{d\theta}{dt} = \frac{V}{L\sin\theta} \tag{70}$$

whereas it is $\frac{2d\theta}{dt}$ at point B with respect to each other.

Assuming that plastic hinges cause a moment *M* per unit weight to resist the rotation of ice floes, Sodhi and Carter (1998) define the rate of energy dissipation E_h at hinges A, B and C as:

$$\frac{dE_h}{dt} = 4M\frac{d\theta}{dt} \tag{71}$$

Equating the rate of work done by externally applied force, *2FV*, to the rate of work operation against the buoyancy forces and energy dissipation within the plastic hinges, it was found by Sodhi and Carter (1998) that:

$$F = \frac{1}{3}\rho g L^2 \cos\theta + \frac{2M}{L\sin\theta} \tag{72}$$

This expression provide an upper bound estimate of the in-plane force by plastic limit analysis under the assumed velocity field, where the vertical movement of point A attributable to changes in water lever is not considered. The first term on the right-hand side is due to buoyancy forces and the second term derives from moments caused by wedging pressure. Sodhi and Carter (1998) point out that in-plane displacement coupled with vertical movement of point A will not produce a wedging action if the two ice floes are in a buckled position between three wet cracks. The probability of thermal ice push coinciding with an event when the ice floes assume a straight position can be very small. Moreover, fluctuations in water level do not allow the cracks to freeze solid, resulting in negligible wedging action.

Therefore, the only term that can results in an in-plane force is buoyancy term alone:

$$F = \frac{1}{3}\rho g L^2 \tag{73}$$

Introducing $\rho g = 9.8kN/m^3$ and the value of *L* given as

$$L = 8.8h^{3/4} \tag{74}$$

the following equation may be obtained:

$$F = 253h^{1.5} \tag{75}$$

The empirical formula by Drouin (1976) for estimation of ice thickness is:

$$h = 0.02\sqrt{S} \tag{76}$$

where h is the ice thickness, m and S is the freezing degree-day accumulation, °C-days.

For normal field conditions, Eq. (75) can be written by applying Eq. (76) as:

$$F = 0.72S^{0.75} \tag{77}$$

where *F,* kN/m is the in-plane force per unit weight () for which the ice floes become unstable by a mechanics similar to buckling.

From Eq. (76)and Eq. (77), the critical pressure, *p*, sufficient to trigger an instability of the floating ice floes may therefore be written as:

$$p = 253h^{0.5} = 35.78S^{0.25} \tag{78}$$

Further, empirical formulas have been presented for three typical structural shapes: vertical dam wall, narrow protruding structure and spillway gate as the following:

- vertical dam wall

$$H_1 = 253h^{1.5} \tag{79}$$

- narrow protruding structure

$$H_2 = \sqrt{\frac{5h}{b} + 1} \times 253h^{1.5} \tag{80}$$

- spillway gate

$$H_3 = e^{-x/a} \times 253h^{1.5} \tag{81}$$

It was suggested that these equations will provide reasonable predictions for the purpose of design under typical conditions of practice. The proposed equations have been confirmed by the data obtained by the Carters et al. (1998).

Later in 2003, Carter (2003) extended the concept of “Indentation” to static ice loads for Dams (this publication is available only in French) which is based on the theory that for piers the effective ice pressure diminished as the contact area increases (CAN/CSA-S471-92). However, the results from some experimental investigations (Morse et al. 2011) showed that the calculated line load (having a peak spatially-averaged value of about 135 kN/m) was more than twice the theoretically possible value as calculated by the Carter et al. (2003).

2.16.Comfort et al. (2003)

A large program was undertaken in Canada from 1991-1992 to 1999-2000 to measure the loads in the ice sheet adjacent to eight dam sites in Manitoba, Ontario, Quebec, and Labrador; to measure the load distribution between the gate and a pier and compare loads on wooden and steel stoplogs. Parallel work was conducted to develop analytical predictors of ice loads.

Comfort et al. (2000) identified the importance of water level fluctuations to the ice loads on dam walls. They found the ice loads to be higher and more variable than those generated by thermal processes alone when there were significant, but not excessive, water level changes. The range of ice thickness during the measurement program was 0.3-0.7 meters. The maximum values of the measured line load resulting from thermal events with negligible change in water level at four dam sites in central and eastern Canada were in the range of 61 to 85 kN/m, with average value of 70 kN/m (Comfort and Armstrong 2001, Comfort et al. 2003). The values resulting from thermal events, combined with significant change in water level at these four dams were in the range of 52 to 374 kN/m, with average value of 186 kN/m (Comfort and Armstrong 2001, Comfort et al. 2003).

According to Comfort et al. (2003) the thermal ice load were comprised of two parts:

- residual load, which are loads that were presented before the start of the loading event
- line load increases produced by ice temperature rises, which result from air temperature rises and/or precipitation, particularly snowfalls.

The equation for predicting the two load components separately is given as

$$LL_{total} = \Delta LL_{ther} + LL_{residual} + LL_{contingency} \tag{82}$$

where LL_{total} is the total line load, ΔLL_{ther} is the line load increase produced by ice temperature changes, $LL_{residual}$ is the residual load in the ice sheet before the thermal event occurred, and $LL_{contingency}$ is a load contingency that was added to ensure that the predicted line loads provide an upper bound to the measured line loads.

Although it was recognized that this approach is not strictly correct from the standpoint of ice rheological behaviour.

Predicting residual loads $LL_{residual}$

$$LL_{residual} = -0.00528A_i + 21.37 \quad (83)$$

where A_i is the ice temperature profile area (in °C·cm) at the start of the event, and $LL_{residual}$ is in kN/m.

Predicting line load increase due to ice temperature rise ΔLL_{ther}

$$\Delta LL_{ther} = 0.064\Delta A^{0.6} h^{0.88} Dur^{f(\Delta A)} \quad (84)$$

$$f(\Delta A) = min\left(log \frac{160}{\Delta A}, 0 \right) \quad (85)$$

where ΔA is the ice temperature profile area change (°C·cm) (Figure 24), h is the ice thickness (cm), and Dur is the event duration (days).

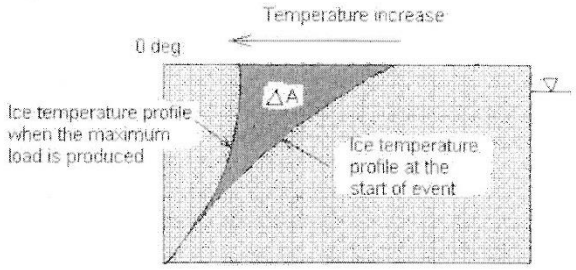

Figure 24. Profile area change definition sketch (Comfort et al. 2003).

The predicted loads obtained by summing ΔLL_{ther} and $LL_{residual}$ were compared with the measured loads to evaluate the degree of fit and the load contingency, see Figure 25.

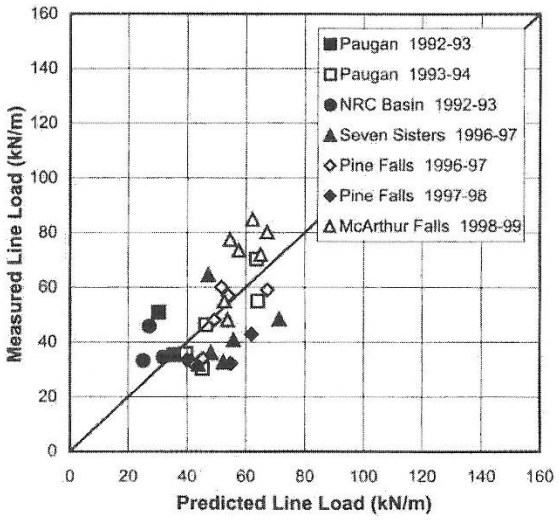

Figure 25. Measured versus predicted total thermal loads (Comfort et al. 2003).

Over the range of available experimental data, the predictive error measured as the difference between the measured and predicted loads, can be approximated by a normal distribution with a mean of - 7 kN/m and a standard deviation of 13 kN/m. The overall range between the predicted load measured values was ± 23 kN/m.

However, the observed range between the measured and predicted loads provides insight. A value of 25 kN/m for $LL_{contingency}$ would ensure that the predicted loads bound the measured loads for all events. A value of 13 kN/m for $LL_{contingency}$ would ensure that the predicted loads exceed the measured loads for 80 % of the events analysed.

Additionally, the total loads due to a combination of ice temperature and water level changes were considered:

$$LL_{total} = \Delta LL_{ther} + LL_{residual} + LL_{waterlevel} + LL_{contingency} \tag{86}$$

where $LL_{waterlevel}$ is the water level change load.

The water level change load contains the following two components: 1) the pure water change water load, which is the load produced solely by a water level change; and 2) the interaction load, which is the second term and models the observed interaction effects (with higher loads being produced when water level and ice temperature changes both took place):

$$LL_{water\ level} = F_1\left[5 + \left(7.5\times10^{-8}\right)\Delta A^2\,\frac{A_i^{1.2}}{Dur^{0.4}}\right] \tag{87}$$

where

$$F_1 = f(\Delta A_i) f(drop) f\left(\frac{a}{h}\right) \tag{88}$$

$$f(\Delta A_i) = \max of \;\; 0 \;\; or \;\; 1 - 4\left(\frac{\Delta A_i}{A_m}\right)^{1.4} \tag{89}$$

$$f(drop) = \max of \;\; 0 \;\; or \;\; 1 - 20\left(\frac{drop}{2h}\right)^{24} \tag{90}$$

$$f\left(\frac{a}{h}\right) = \left[\frac{1}{\max \;\; of \;\; 0.22 \;\; or \;\; a/h}\right]^2 \tag{91}$$

and *A* is the average water level change amplitude (absolute value, cm) over 2-3-days leading up to the peak load; h is the reservoir ice thickness (cm); ΔA is the profile area change (absolute value, °C·cm); ΔA_i is the initial profile area change prior to the start of the event (absolute value, °C·cm); A_i is the temperature profile area at the start of the events (absolute value, °C·cm); drop is the drop or rise in mean water level during the event (absolute value, °C·cm); and A_m is the maximum ice temperature profile area (°C·cm), which was defined as $20 \times h$ (in cm).

Although residual loads were affected by several parameters the ice thickness and the ratio a/h were found to have the greatest effect. The data were scattered, the following trends are evident: residual loads were larger in thicker ice and the residual loads decreased as the ratio a/h was increased.

The best fit equation for the residual loads $LL_{residual}$ (kN/m) with respect to these parameters is shown in Eq. (92), which predicted the measured residual loads within 29 kN/m.

$$LL_{residual} = 0.37 f(h) + \frac{1.47}{a/h} \tag{92}$$

with

$$f(h) = h - 25 \;\; \text{for} \;\; h > 25 \tag{93}$$

where h is the ice sheet thickness (cm).

It should be noted that Eq. (93) is not applicable for $h \le 25$cm.

Eq. (92) will always produce positive values for the residual load, indication that the residual loads are compressive. Some of the measured residual loads were slightly negative, suggesting that there was a small amount of tension in the ice sheet. This probably resulted from cooling of the ice sheet at the time when the next event started. This was not accounted for in developing the ice load algorithms because the measured load tensions were small, and this approach errs conservatively.

The variation between the measured and predicted loads was generally similar in magnitude over full range of data. As result, the prediction error is smallest, on a per cent basis, for the highest loads, which are the loads of greatest concern. Over the range of data, the difference between the measured and predicted loads is normally distributed with a mean of 0 kN/m and a standard deviation of 45 kN/m. it was also noted that negative errors are of most concern, as these represent the case where the ice load algorithms under predict the measures loads. The probability that the algorithms under predict the measured loads by less than 60 kN/m is 90 %.

2.17. Ekström (2006)

Ekström (2006) presented a mathematical and a numerical model of ice loads on structures. In this work, a continuum model is used, despite the drawbacks in fracture phenomena around cracks. Additionally, to the fact that no creep effects are not applied in this model.

The ice is assumed to be isotropic. Below the yield limit the ice is assumed to behave linear elastic and above perfectly plastic. The stress σ – strain ε relation is assumed as:

$$\boldsymbol{\sigma} = \boldsymbol{D}\left(\boldsymbol{\varepsilon_{el}} + \boldsymbol{\varepsilon_{pl}}\right) + \boldsymbol{\sigma_0} = \boldsymbol{D}\left(\boldsymbol{\varepsilon} + \boldsymbol{\varepsilon_{th}} + \boldsymbol{\varepsilon_0} + \boldsymbol{\varepsilon_{pl}}\right) + \boldsymbol{\sigma_0} \tag{94}$$

where $\boldsymbol{D}$ is elastic matrix, ε_{el} is elastic strain vectors, ε_{th} is thermal elastic strain vector, ε_{pl} is plastic strain vector and σ_0 is initial stress.

A Drucker-Prager condition was used in the presented model to calculate when the stress reaches the yield limit. The same basic principles are used for modelling of concrete.

3. Comparisons of the measured and calculated results

The first approximation of thermal ice loads at different locations and climatic zones was done on the basis of available empirical values. The maximum measured ice load acting on the surface on the dam face, i.e., 370 kN/m, was registered in Canada, while several measurements showed an average ice load of 150 - 200 kN/m.

The first reported field investigations including in situ measurements of ice pressure showed seasonal maximum of 240, 200 and 300 kN/m (Fransson 1988). Also laboratory tests were carried out in order to simulate expansion with complete restraint. The maximum thermal ice pressure of 250 kN/m has been measured during the laboratory experiments by Löfquist (1954) in Sweden.
The laboratory test series showed higher maximum pressures than the field measurements. However, the used rates for the temperature change during the laboratory experiments were considerable higher than usually expected in a thick ice cover in the field. A summary of results of some full scale and model measurements (carried out before 1984) was presented by Löfquist (1987) and can be found in Table 1. The maximum values of the thermal ice load are between 100 - 507 kN/m.

Drouin (1970) made a comparison between results obtained by some of the theories using specific conditions that the initial temperature of ice - 40°C is raised at rate of 2.8 °C/hour, the ice cover is uniaxial restricted and without a snow cover, and no solar energy is absorbed. Later the list of the results tabulated by Drouin (1970) was extended by Kjeldgaard (1977) and Bergdahl (1978), see Table 2.

However, as it was pointed by Timco et al. (1996) that these early measurements were plagued with poor measuring instrumentations, so obtained results were not generally reliable. More recently, there have been a number experiments performed to measured thermally-induced stresses using more sophisticated instrumentation. Also these later experiments used instrumentation at different depths within the ice sheet, so pressure distributions could be determined. This produces a much more accurate estimation of the thermal load.

Comparison of five theories (Rose 1947; Russian Code SN-76-66 (1973); Drouin and Michel 1974; Xu Bomeng 1981, 1986; Fransson 1988) performed by Timco et al (1996) , see Figure 26, with available field data measured at the NRC outdoor basin (Canada) in winter 1993 and at the Paugan Dam (Quebec) during winters of 1993 and 1994, showed a poor correlation between the calculated and measured values. None of these models for predicting ice pressure was capable of predicting the measured pressure within an acceptable margin of error (Timco et al. 1996). The difference between theoretical estimates and measured values of loads on dam walls may be attributed to changes in water levels in reservoirs and large wet cracks in the ice cover.

Later in 1999, Timco et al. (1999) presented a summary over a number of wide structures in Canada (Baffin Island and Ottawa) which have been instrumented to determine the ice loads, mostly due to a thermal origin. In all cases, the structures were quite wide, on the order of 75 to 100 m, and surrounded by landfast ice. In total, 42 events have been extracted and these events were on the order of several hours to several days. The width of these structures ranged from 97 to 124 m. Measured loads ranged from 0.4 to 16.9 MN, due to ice with a thickness that ranged from 0.17 to 1.45 m. (Timco et al 1999).

Results of in situ measurements of ice loads on Silvann dam in Narvik (Norway) during winter 1998-1999 were presented by Hoseth and Fransson (1999). The maximum measured ice load was 135 kN/m with ice thickness of 0.6 m. A semi-empirical equation by Fransson was used to estimate the thermal ice loads. Comparison of the measured and estimated values showed a good agreement with previously performed measurements in Sweden.

Finally, as s it was mentioned before in this report, results from some experimental investigations in Canada (Morse et al. 2011) carried out during last years, showed that the calculated line load (having a peak spatially-averaged value of about 135 kN/m) was more than twice the theoretically possible value as calculated by the Carter et al. (2003). This suggests that the nature of the fissure near the dam may be very important in predicting possible maximum loads as it may affect the nature of the instability in the ice sheet.

Table 1. Maximum thermal ice load (Löfquist 1987).

Authors	**Publication year**	**Ice pressure, kN/m**	**Ice thickness, m**
Royen	1922	300	1.0
Löfquist; model experiment	1954	250	0.6
Monfore; field investigations	1954		
Winter 1947-1948		240	about 0.5
Winter 1948-1949		210	about 0.5
Winter 1949-1950		300	about 0.5
SOU 1961:12	1961		
for bridges		100-200	-
for dams		100-200	-
for dams, exceptions		100-400	-
Lindgren	1968	460	0.6
Bergdahl; calculated maximum for 100 years period in the lakes, Sweden	1978		
Torne träsk (Norrbotten)		507	
Runn (Dalarna)		410	
Vidösten (Småland)		330	
Fransson and Cederwall, calculated from measurements in the natural ice floe next to the bridge piles	1984		
		300	1.0
		220	0.5

Table 2. Thermal ice load computed by different theories (Tsinker 1995).

Source		**Ice force, kPa, for ice thicknesses**	
		0.45m	0.9m
Rose (1947)[a]		47	86
Monfore (1954)[a]		222	232
SN76-59 (1959)[a]		128	255
Drouin and Michel (1971)[b]	S1 ice	330	390
	Snow ice	220	270
SN76-66 (1966)	0 m/s	30	60
	5 m/s	310	440
	20 m/s	410	580
Bergdahl (1978)	0 m/s	459	752
	5 m/s	502	830
	20 m/s	531	829

[a] Calculated from Drouin (1970)

[b] Calculated from Kjeldgaard (1977)

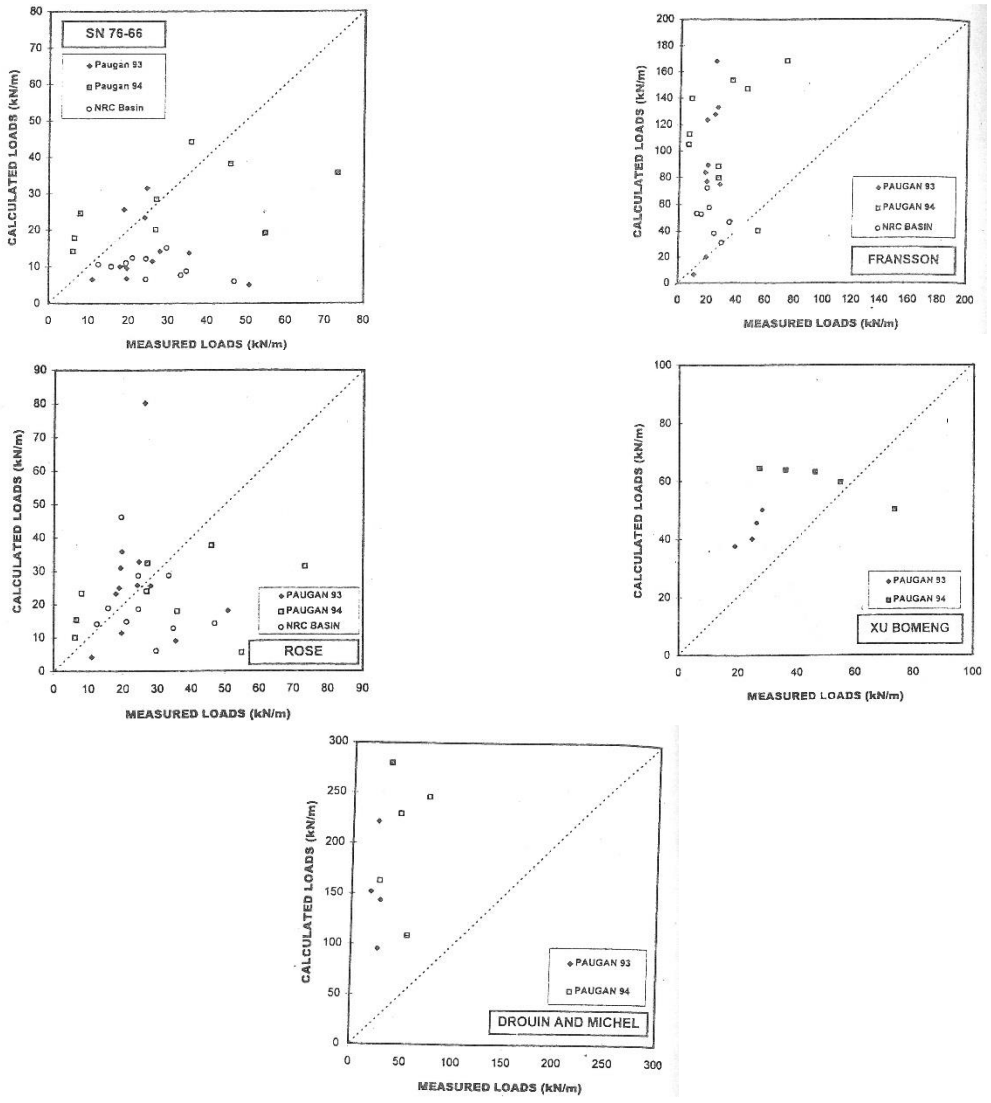

Figure 26. Comparison between measured and calculated results using the theories by theories Rose

1947; Russian Code SN-76-66 (1973); Drouin and Michel 1974; Xu Bomeng 1981, 1986; Fransson 1988 (Timco et al. 1996).

4. Ice load values, current standards and recommendations

4.1. USA

Previously in Design Criteria for Concrete Arch and Gravity Dams (1977) the method of Monfore and Taylor (1948) was suggested for using to analyze anticipated ice pressures if necessary basic data are available. An acceptable value for the ice load of 146 kN/m can be expected on the face of a structure for an assumed ice depth of 0.6 meter or more when basic data are not available to compute pressures.

Kocahan and Rodionov (2003) mentioned that 150 kN/m are suggested for 25 inch (0.64m) thick ice, and 220 kN/m for 35 inch (0.9 m) thick ice.

The method of calculating thermal ice load in a confined ice sheet is presented in the report by U.S. Army Corps of Engineers EM 1110-2-1612 (Engineering and Design - Ice Engineering 2002), and for an unconfined case, see Sanderson, (1988). Calculations of typical thermal ice load are in the range of 200–400 kN/ m, whereas some of the measured values are in the range of 100–350 kN/m (Sanderson 1984).

Except for the recommended values of effective pressure, the guidelines by U.S. Army Corps of Engineers for ice loads on structures are almost the same as those of the American Association of State Highway and Transportation Officials (AASHTO 1994), which in turn were adopted from the Canadian Standards Association (CSA 1988, 2000). The CSA (2000) and the AASHTO (1994) codes consider dynamic and static loads on bridge piers located in rivers, lakes, and coastal waters. The static loads are generated by thermal expansion or contraction of the ice and by fluctuations in the water levels.

Some information about vertical loads is also could be found in the report by U.S. Army Corps of Engineers EM 1110-2-1612.

4.2. Canada

In recommendations by the Canadian Department of Environmental (1971) it is assumed that the ice pressure varies linearly with ice thickness, and therefore recommended loads of 150 and 220 kN/m subsequently correspond to ice thicknesses of 0.3 m and 0.6 m, respectively. In an overview presented by Tsinker (1995), and later by Kocahan and Rodionov (2003), values for the the ice pressure are between 150 to 220 kN/m for fixed structures and 70 -75 kN/m for more flexible structures.

According to "Water control structures selected design guidelines" (2004) traditional values generally considered suitable for static ice loads acting on a unit width of a dam or similar structures are as follows:

- 150 kN/m (10 kips/ft) for concrete dams and structures
- 75 kN/m (5 kips/ft) for steel gates
- 30 kN/m (2 kips/ft) for timber stop logs

The ice thickness is normally considered to be 0.6 m thick with the ice load acting at 0.3 m below the water level.

Recent studies on static ice loads for dams, conducted by Comfort et al. (2003), suggest that considerable higher ice loads than traditional values can occur when significant, but not excessive, changes in reservoir levels are expected.

The National Research Council of Canada in Ottawa has developed an “Ice Load Catalogue” (Timco and al. 1999). This catalogue contains over 300 events of ice loading on offshore and coastal structures. The catalogue contains information on the time-based behaviour of the load as well as details of the ice conditions during each loading event. There is a complete range of structures that are included in the Catalogue including bridge piers, light piers, wharves, dams, offshore structures and natural islands.

Comfort et al. (2003) have developed methods for prediction of ice load. The presented algorithms predicted thermal loads well, but they are less accurate for loads produced by a combination of water level and ice temperature changes. In the work presented by Comfort et al. (2003) the thermal ice loads were comprised of two parts: residual loads, which are loads that were present before the start of loadings event; and a line load, which increases due to ice temperature rises and/or precipitation, particularly snowfalls. To determine the ice loads generated by a combination of ice temperature and water level changes "water level change load" was additional added to the residual loads and "pure thermal loads".

Stander (2006) presented the data collected at La Gabelle reservoir located in south-central Quebec, Canada, during the winters of 1992 and 1993. It was documented the increase in stress (about 100 to 200 kPa) due to a rise in water levels and showed that stress increased by about 4-5 kPa/ cm rise in stage height and were superimposed on thermal stresses , providing a maximum ice thrust on the order 20-25 t/m at the measured ice thickness of 0.75 m. He also noted that the process of tidal jacking led to displacement of the ice sheet away from the dam (at a rate of around 8 mm/day), and that ice growth within the fissures was the root of the process. He further noted that stresses created by this process were attenuated over short distances by the ice sheet itself.

A program to evaluate ice load thrust on dams was undertaken during winters 2007-08 at La Gabelle, 2008-09 at Beaumont and La Gabelle, and during winter 2011 at Barrett Chute in Canada. The main objective was to measure ice load thrust on the dam face in order to harmonize different design load criteria. It was also presented a comparison of the recorded near and far-field ice thrust as well as results obtained from different measuring systems. Only results from experimental measurements and observations (no theoretical approach) are presented by Morse et al. (2009), Taras et al. (2009), Morse et al. (2011) and Taras et al. (2011).

Morse et al. (2009) and Taras et al. (2009) reported similar findings over subsequent winters at La Gabelle, and generally confirmed Stander’s observations. They also demonstrated a large spatial-temporal variability of stresses along the dam face. They postulated that stresses may be controlled by the rate of strain occurring in

the ice sheet. Strains are generated by water level changes, with a lesser, but significant contribution from thermal expansion. Morse et al. (2009) pointed out, that in order to know the real average pressure on the dam, a significant amount of panels are required. It was shown that the estimated maximum average unit force on the dam (92 kN/m estimated from our 12 panels) could be significantly over- or under-estimated if there are insufficient panels to know how the loads are distributed. For example, if only 1 panel was placed on the dam, depending on its location, it would have measured no force at all or it may have measured a peak value of 180 kN/m. Had 5 panels been placed on the dam, depending on their location, the estimated maximum force would have varied between 25 to 160 kN/m. For 9 panels, it would have been between 70 and 120 kN/m. This fact has important implications for determining safe design values.

Taras et al. 2011 presented results of measurements of ice loads by three different types of sensors (Carter panels, BP gauges and Biaxial gauges) which were used in field during the last twenty years. Ice stresses were recorded at different depths in the ice sheet against or near the wall and at sites 5 m and 30 m away from the wall. Line load obtained from the three types of sensors tracked each other quite well and values are within the uncertainties. Significant ice load values (greater than 100 kN/m) were obtained for both dams during the 2011 winter. The averaging of loads measured over a 25 m linear face of the dam reduced the peak load but was still 30% larger than in the far field.

Morse, (2011) the present data set from Barrett Chute does generally compliment findings published by Stander (2006), Morse et al. (2009) as well as Taras et al. (2009) and some other. However, in contrast to the previous reports from 2009, the 2011 ice loads were primarily thermally generated. In addition, the events of interest did not occur over a few days (as was observed previously) but rather over 6 to 8 hour periods. The amount of rise measured here was on the order of 5.8 kPa/cm (as compared to 4 kPa/cm found previously at La Gabelle). However, the overall effect at Barrett is considerably less than that at La Gabelle, where water level fluctuations average four times that observed at the former site. Similarly, it was found that the fissure near the dam face at Barrett Chute grew by about 3.6 mm per day (5 mm during the heart of winter) as compared to 8.0 mm/day at La Gabelle. The data also show that quick thermal events (6-8 hours) can be significant (whereas previous field campaigns suggested that slow events (2-4 days) were the most important). Data here suggest a consistent rise of 80 kPa per degree Celsius rise in ice temperature. It was also shown to be independent of the rate of thermal increase. Events were generated by local flooding events, as well as global changes in air temperature. The data also suggest that the spatial variability of stress was much greater for water level induced events than to thermal events.

Finally, the stresses were much greater (stresses up to 350 kPa) than those previously observed during thermal events. It was presented that for the ice sheet approximately 0.4 m thick, the line loads generated top out at 140 kN/m. It should be noted here that previous thermal line loads reported by Comfort et al. and those estimated by Carter's analysis suggest that an ice sheet should not be able to support more than 60 kN/m, see Eq. (79), prior to failure.

Based on the work by Comfort et al. 2003 an Ice Loads Design Guide (Static Ice Loads On Hydro-Electric Structures 2003) was produced synthesizing the results obtained from various previous years, and establishing a statistical database that allows ice loads to be calculated in a coherent format for the long face of dam for various locations, water level change operational regimes, return periods and confidence levels. These ice loads

would be applicable to dam safety analyses. Stoplogs for various design cases may be also calculated using this Guide.

Some information on vertical ice loads can be obtained from CAN/CSA-S6-06, Canadian Highway Bridge Design Code and S6.1-06, Commentary on CAN/CSA-S6-06, Canadian Highway Bridge Design Code.

4.3. Sweden

The values of the thermal ice loads in Sweden depend on the geographical regions and are in the range of 50 and 200 kN/m (RIDAS 2008). In the south part of Sweden the value of 50 kN/m is used for Skåne, Blekinge, Halland, Bohuslän and Västergötland regions (fylke). Up to the line between Karlstad and Stockholm the values of 100 kN/m are recommended, and over this line, the values of 200 kN/m are suggested when considering the stability of dams. The ice loading mechanisms and statistics on ice conditions in Swedish seas (ice thickness, ice period etc.) were presented in the recommendation by Fransson and Bergdahl (2009).

4.4. Norway

In NVE (2003) it is suggested that the values of the thermal ice load in Norway are normally between 100 kN/m and 150 kN/m acting at 0.25 m below the higher water level (NVE 2003). According to NVE (2003) the values of 100 kN/m can be used without any considerations for dams in low durability class. The values lower than 100 kN/m can be accepted in special cases if the reason for these values is presented. For example, ice pressure lower than 100 kN/m can be used for dams and some technical installations (gates) with a thermal heating system and with properly performed installation of the control equipment.

In cases where the frequent water level fluctuations in the magazine occur, the combined ice pressure can be significantly larger than the thermal ice pressure. This could be applied, for example, for reservoirs and river power stations with day variations greater than ± 0.2 m. According to the Norwegian recommendations, the load will then largely depend on the ice, i.e. the amount of frost, and the upper limit of ice action can such cases is simply set to:

$$P_{ice\_\max} = 250 \cdot h^{1.5} \quad (945)$$

where h is ice thickness, m.

The maximum ice thickness is suggested to be equal:

$$h_{\max} = 0.02 \cdot F^{0.5} \quad (96)$$

where F is amount of frost, °C days. Summary of amount of frost in the different regions of Norway could be found in the publications and manuals by Vegdirektoratet.

In some international publications (Kjeldgaard and Carstens 1980, Tsinker 1995) the values of ice load of 100 kN/m for an average ice condition and 150-200 kN/m under especially unfavourable conditions are presented as typical values for Norway. Previously in 1970 the values of ice pressure 20 - 90 MPa for Norway and 150-200 MPa for Sweden were given by Starosolszky (1970).

The regulations for the safety of water systems have until now been collected in a "Safety Guide for Water Systems" (in Norwegian - Sikkerhetshåndbok for vassdragsanlegg). In 2010 the new Dam Safety regulations came, which replace the previous versions of the regulations, and some of specific provisions from other guidelines.

A research project has been carried out in Norway (EBL Kompetanse 2002). A literature study, in situ measurements of ice loads on Silvann dam in Narvik in the Northern Norway during winter 1998-1999 and re-calculations of eight dams were presented in the research report. The measured ice loads on Silvann dam ranged from 50 to 135 kN/m with ice thickness that ranged from 0.51 to 0.62 m (Hoseth and Fransson 1999).

Ice pressure measurements in a small Treserviour at Taraldsvikfossen, also near Narvik , have been ongoing since winter season 2012-2013. The reservoir is located 213 m above sea level and has a surface area of approximately 1000 m2, is not in service and maintained as a back-up for drinking water supply. It is confined by a straight-sided concrete dam, 6 m high. A fraction of the waters of a creek, Taraldsvikelva, enters the reservoir during most of the year, keeping the water in the reservoir at the level of the spill way. The water level is 0.5 m below the dam surface, except during surges (Petrich et al. 2014). Ice forms in the reservoir each year in fall and persists through approximately May, with the highest loads seen typically during the first three months of a year (https://ndat.no/dam/).

Pressure cells were frozen into the ice and recorded both compression and, to a limited degree, tension. Different configurations and locations of the cells along the dam and in the entire reservoir were presented.
Recorded pressures at a single measurement cell ranged from about 0.2 MPa in compression to -0.1 MPa in tension for the thermal loading. Various effects resulted in stresses at the reservoir, including thermal expansion and water level fluctuations or other mechanical events, are presented. The dominance of one or other, or the combination of those processes varied between seasons (Petrich et al. 2014; Petrich et al. 2015, Petrich et al. 2016, O'Sadnick et al. 2016). Unfortunately, the values of the line load are not clearly presented. The preliminary calculated line loads are around 100 kN/m (Petrich and Arntsen 2018) and, based the data available from the web-site (April 2019 , https://ndat.no/dam/), do not exceed 150 kN/m.

An attempt to present trends and regional differences in thermal ice loads on dams which are expected to be significant in Norway, was made by Petrich and Arntsen (2018). According to presented estimations, locations with less than freezing degree days of 500 °C days are expected to see seasonal maximum lines loads rarely exceeding 100 kN/m, while locations with less than 800 °C days will rarely exceed 150 kN/m. With the exception of reservoirs at a few locations, 200 kN/m are expected to be rarely exceeded anywhere in Norway in the 2010s. The highest line loads are expected in Northern Norway, in particular in the plateaus of Finnmark. Other areas of significant line loads lie in the mountains along the Norwegian-Swedish border and inland in Southern Norway. Reservoirs near the coast and East of the mountains see low to moderate ice loads. The long-term trend is toward lower ice loads. The regional dependence of the magnitude of the trend is non-trivial, suggesting changing climate has regionally different fingerprints throughout Norway.

4.5. Russia

The comparison of calculated results with measured data has been performed by Timco et al. 1996 using among others the Russian recommendation SN-76-66 which is almost 50 years old. Russian standard SNiP 2.06.04.82 (1995) originating from river ice actions on bridge piers is an updated version of SN-76-66. Previously, SNiP 2.06.04.82 (1995) was applied to offshore applications.

Overview over past and current Russian standards, guidelines and recommendations are presented below.

Previous versions of the Russian Standard:
[1] Guidelines for determination of river ice loads on structures СН 76-66 -1966 - Указания по определению ледовых нагрузок на речные сооружения СН 76-66 - 1966
[2] Loads and impacts on Hydraulic structures (from waves, ice and ships) SNiP II-57-75 – 1976 -Нагрузки и воздействия на гидротехнические сооружения (волновые, ледовые и от судов) SNiP II-57-75 – 1976
[3] Loads and impacts on Hydraulic structures (from waves, ice and ships) SNiP II-57-75 – 1982-Нагрузки и воздействия на гидротехнические сооружения (волновые, ледовые и от судов) SNiP II-57-75 – 1982
[4] Loads and impacts on Hydraulic structures (from waves, ice and ships) SNiP 2.06.04-82* - 1982-Нагрузки и воздействия на гидротехнические сооружения (волновые, ледовые и от судов) SNiP 2.06.04-82*
[5] Loads and impacts on Hydraulic structures (from waves, ice and ships) SNiP 2.06.04-82* - 1995 (not approved version) -Нагрузки и воздействия на гидротехнические сооружения (волновые, ледовые и от судов) SNiP 2.06.04-82* - 1995

Current Russian version:
[6] Loads and impacts on Hydraulic structures (from waves, ice and ships) SNiP 2.06.04-82*, SP 38.13330.2012 – 2014

Additionally:

Р 31.3.07-01. Guidelines for the calculation of loads and impacts from waves, ships and ice on sea hydraulic engineering constructions, 2001 -Р 31.3.07-01. Указания по расчету нагрузок и воздействий от волн, судов и льда на морские гидротехнические сооружения, 2001

Text STO Gazprom 2-3.7-29-2005 method of calculating ice loads on the ice-resistant fixed platform -Текст СТО Газпром 2-3.7-29-2005 Методика расчета ледовых нагрузок на ледостойкую стационарную платформу.

Using SNiP 2.06.04.82 (1995), the horizontal thermal ice load could be calculated as a function of the air temperature difference and corresponding "reduction ice thickness". This reduction ice thickness could be estimated as a sum of snow thickness, average ice thickness measured during the period of changing in the air temperature and additional thickness of ice depended on wind velocity. Ice load acts at 0.25hc m below the water level, where hc is an average ice thickness measured during the period of changing in the air temperature.

Vertical ice loads by SNiP 2.06.04.82 (1995) can be determined as a non-linear function of the maximum ice thickness and the water level changes. It should be noticed that the updated version of SNiP 2.06.04.82 (1995)

contents a simplified approach for estimation of both horizontal and vertical loads compared to the previous version SNiP 2.06.04.82 (1982).

Recommendations CO34.21.145-2003 (applied from July 2005) presents only an updated approach for calculations of dynamic loads on the hydro-electrical structures and bridges from moving ice floe and ice ridges.

The last version SNiP 2.06.04-82*, SP 38.13330.2012 – 2014 [5] gives the guidelines for calculation of:

- Horizontal ice load (MN/m) due to the thermal expansion (paragraph 7.13)
- Vertical ice load (MN/m) due to change in the water level
- Estimation of line ice load by SNiP SP 38.13330.2012 – 2014

The horizontal line load_in MPa/m2 due to the thermal expansion could be obtained by the graphical representations presented on the figures in SNiP 2.06.04-82* - 1995 and SP 38.13330.2012 – 2014.

The values should be selected based on three parameters: values of the change in the air temperature (-10C, -20C, -30C), the average ice thickness *hi* at the time of the considered thermal event and the apparent ice thickness h_{app}. The interval of the air changing should not be less than 5 hours and not more than 20 days.
The apparent ice thickness could be estimated as:

$$\boldsymbol{h_{app} = h_i + 1.43 \cdot h_s + h_{add}} \quad (957)$$

The values of the additional ice thickness h_{add} could be found in Table 3 for different values of the air temperature changing and the average wind speed, m/s. The values of the additional ice thickness could be found in the table for the case when ice is covered by snow and for different wind speed values (1-10 m/s).
The total line load in kN/m could be found from Figure 27.

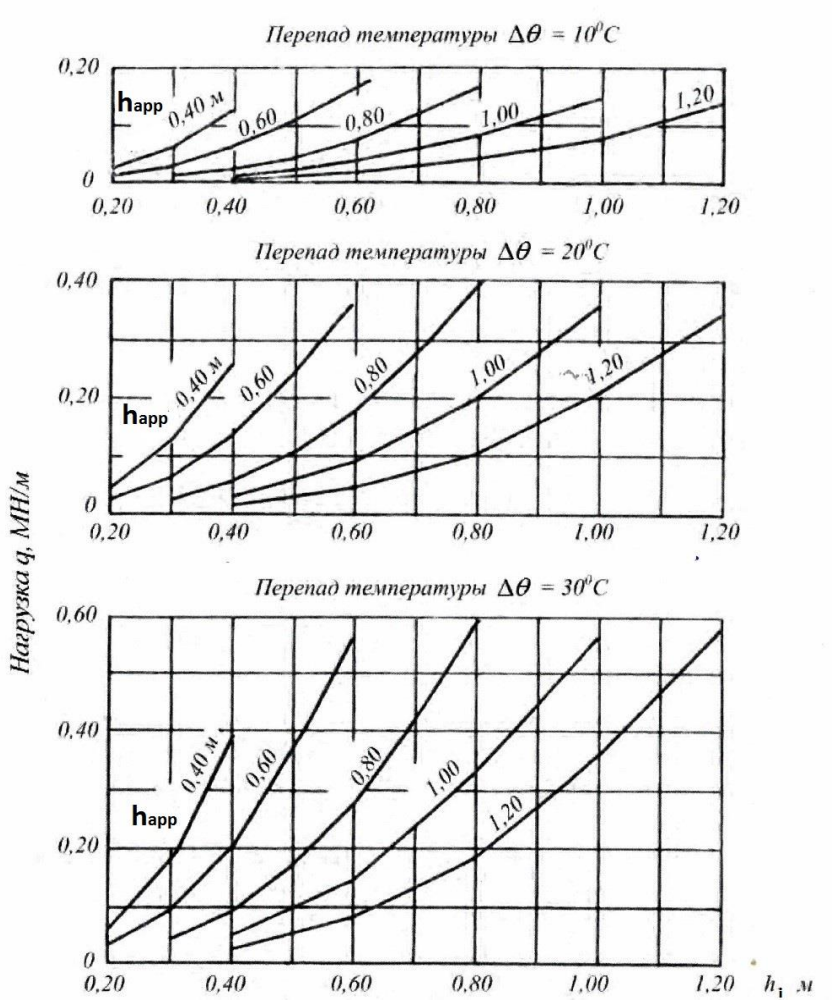

Figure 27. Estimation of line ice load (SNiP SP 38.13330.2012 – 2014).

Table 3

Средняя скорость ветра V_w, м/с	Добавочная толщина льда h_r, м, при средней температуре воздуха θ_a и наличии снега на льду			
	0°	–10°	–20°	–30°
1	0,46	0,45	0,45	0,45
3	0,15	0,15	0,15	0,15
5	0,09	0,09	0,09	0,09
10	0,046	0,045	0,045	0,045

Previous versions of the Russian standard (SNiP 2.06.04-82*, SNiP II-57-75) include some of the mathematical basic for calculation of the thermal loads.

- Estimation of line ice load by SNiP 2.06.04-82*-1982

According to SNiP 2.06.04-82*, the line load (MN/m) on the structure due to the thermal expansion of ice (salinity less than 2‰) could be determined by following formula:

$$\boldsymbol{q = h_{max} k p_t} \quad (98)$$

where h_{max} is maximal ice thickness in m, *k* is coefficient dependent on the length of the ice edge and p_t is ice pressure in MPa.
The coefficient k is set to unit for the ice length less or equal to 50. For the ice length of 70, 90 and 120 m, the coefficients are 0.9, 0.8, 0.7, respectively. For the ice length of 150 m and more, the coefficient is 0.6.
Then the ice pressure, MPa, is calculated as sum of elastic and plastic deformations:

$$\boldsymbol{p_t = 0.05 + 11 \cdot 10^{-5} \nu_{t,a} \eta_i \varphi}, \quad (99)$$

where $\nu_{t,a}$ is maximum change of the air temperature for 6 hours, η_i is coefficient of ice viscosity and φ is dimensionless parameter determined by the graphs in the standard, see Figure 28. The coefficient of ice viscosity η_i could be determined by equations:

for $\boldsymbol{t_i \geq -20}$℃ : $\boldsymbol{\eta_i = (3.3 - 0.28 t_i + 0.083 t_i^2) 10^2}$ (100)

for $\boldsymbol{t_i < -20}$℃ : $\boldsymbol{\eta_i = (3.3 - 1.85 t_i) 10^2}$ (101)

where t_i is the temperature of ice, ℃, calculated by:

$$\boldsymbol{t_i = t_b h_{rel} + \frac{\nu_{t,a}\, t}{2} \psi} \quad (102)$$

here: t_b is initial air temperature, ℃
t is time interval, h, between two measurements of air temperature
h_{rel} is relative thickness of ice covered by snow, m:

$$\boldsymbol{h_{rel} = \frac{h_{max}}{h_{red}}} \quad (103)$$

h_{red} is apparent ice thickness, m, which could be estimated as:

$$\boldsymbol{h_{red} = h_{max} + 1.43 \cdot h_{s,min} + \frac{2.3}{\alpha}} \quad (104)$$

where
$h_{s,min}$is minimum snow thickness for considered time, m, based on the measurements. Otherwise, the $h_{s,min} = 0$

α is coefficient of thermal conductivity (at the air-snow surface), W/m2, estimated by empirical formulas:
With snow :

$$\boldsymbol{\alpha = 23\sqrt{v_{w,m} + 0.3}} \quad (105)$$

Without snow :

$$\boldsymbol{\alpha = 6\sqrt{v_{w,m} + 0.3}} \quad (106)$$

where $v_{w,m}$ is average weed speed, m/s.
ψ is dimensionless parameter determined by the graphs in the standard, see Figure (28)

Both ψ and φ could be estimated using the apparent ice thickness h_{rel} and factor F_0:

$$\boldsymbol{F_0 = \frac{4 \cdot 10^{-3} t}{h_{red}^2}} \quad (107)$$

Load due to the inclined side of the structure (angles less than 40^o) could be ignored.

For salinity ice $S \geq 2‰$, the line load could be estimated by equation (96) using the ice pressure value $p_t = 0.1$ MPa.

No values of typical thermal or vertical ice loads are presented in the Russian Standards. In some literature sources (Starosolszky 1970, Tsinker 1995 and Kocahan and Rodionov 2003) it was mentioned that in Siberian regions of Russia ice pressure of 300 kPa was commonly used whereas for somewhat less severe conditions, such as Caucasus and St. Petersburg region, ice pressures ranging from 150 to 200 kPa are common used.

Assume the air temperature is changed from to 0 C to - 10C ($\Delta\theta = 10°C$), duration of the thermal event is 6 hours, the ice thickness *hi* is 0.8 m, wind speed is 1m/s and no snow on the ice surface. Based on the curves in the SNiP SP 38.13330.2012 – 2014, the thermal ice load is estimated to be about 160 kN/m. Unfortunately, in the case of the show cover of 10 cm, the line ice load could not be estimated by the graphs because of the average and apparent ice thicknesses in the graphs presented only up to 1.2 m, but the calculated value of *happ*=1,4 m in the current example. If the speed of wind is suggested to be 5 m/s, the estimated ice load is under 100 kN/m.

The line ice load was also calculated by SNiP 2.06.04-82* - 1982. As presented in Table 4, the values of calculated line ice loads are under 50 kN/m. As it could be seen from this example, the values of ice loads calculated by SNiP 2.06.04-82* - 1982 are much lower than values obtained by new Russian standard. However, the background for the curves in Figure 27 are not presented.

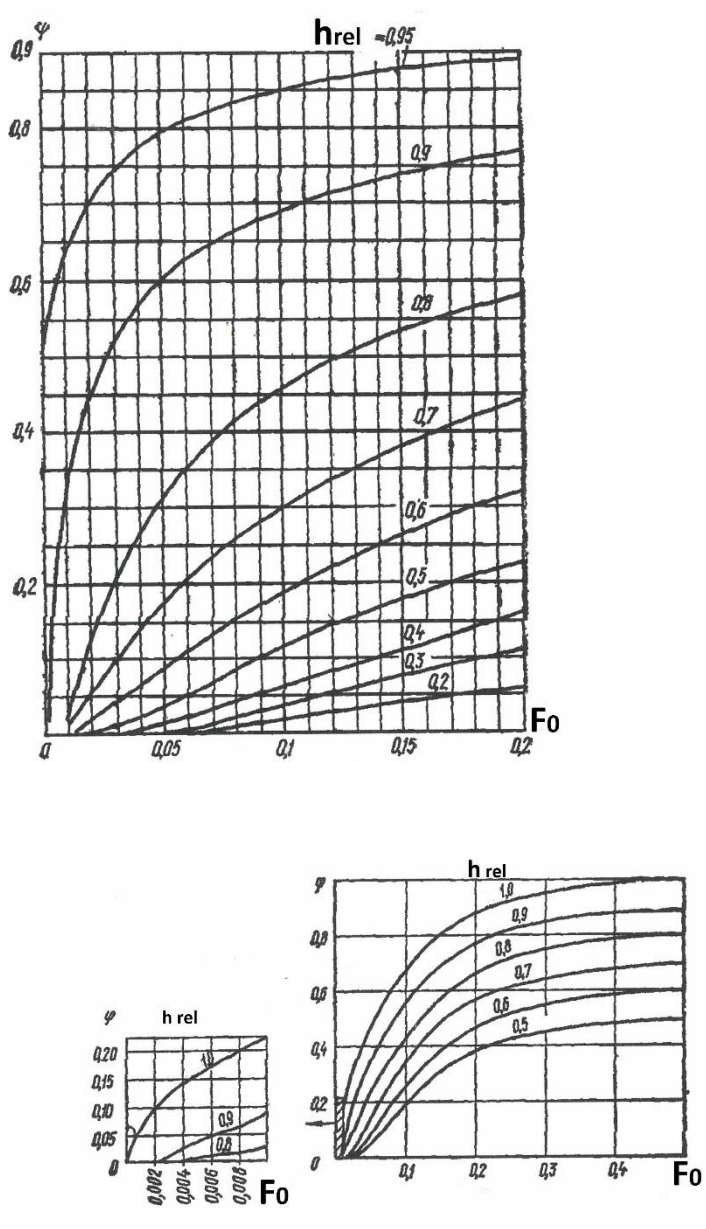

Figure 28. Estimation of the paraments in the model (SNiP 2.06.04-82-1982).*

Table 4 Line ice load calculated by SNiP 2.06.04-82 - 1982*

	Without snow	With snow
hmax, m	0.8	0.8
hred,m	1.14	1.03
hrel ,m	0.70	0.78
F0	0.0186	0.0226
ψ	Approx. 0.05	Approx. 0.13
φ	Approx. 0.01	Approx. 0.05
Ice pressure kN/m2	51.7	58.7
Line ice load kN/m	**41.3**	**46.95**

4.6. Other countries

Finland
A Finnish Guideline for the loads of structures (Finnish RIL-144, (2001) is mentioned in some publications. However, this standard is available only in Finnish, and currently, no information in English have been found about values and calculation models for determination of the thermal ice loads.

Austria
According to EBL Kompetanse report (2002), the ice load on the dam can be estimated as 146 kN/m based on the criterion which is suggested for the design phase. However, for safety calculations and other analyses during drift operation of the dams, the ice loads on the dam face can vary between 14- 48 kN/m.

Japan and China
In the EBL Kompetanse report (2002) it was mentioned that the comparison of the thermal ice load for different countries including Japan and China, was also presented by Billfalk et al. (1996). Unfortunately, this comparison contents some errors and incorrect information.

5. Summary

An ice sheet will expand when it is subjected to an increase in temperature. During winter time, the air temperature continually changes, and as results, ice sheet expansion leads to a load on structures. Knowledge of the level of load is important for the design of hydroelectric dams and water storage reservoirs.

The first approximation of the thermal ice loads at different locations and climatic zones was traditionally done on bases of available empirical values. Several theories have been proposed to calculate the thermal ice loads but, unfortunately, the comparison of some models with measured data showed a wide disparity, and no model predicted the measured loads (Timco et al. 1996).

The basis for the calculation of the stress and strain in the ice can be a rheological equation where the rate of strain is given as a function of stress and the rate of change of stress. Furthermore, the rate of strain is a function of the rate of change of ice temperature. When the strain rates at different levels of the ice cover and the rheological model for ice are known; and calculation of the temperature variation is presented, the thermal pressure can be computed numerically step by step. So, generally it seems that there are two main steps towards the estimation of thermal ice pressure are estimation of the ice temperature or its derivative and calculation of the stress-strain state in the ice.

Already in 1922, Royen (1922) proposed a simple analytical expression of the maximum pressure as a function of initial temperature and the rate of the temperature rise. The creep law suggested by Royen was based on experimental creep curves, and the temperature is assumed to be uniform over the ice thickness.

Several experimental investigations were carried out in the period until 1960, and the results of these experiments were usually summarized in graphs and diagrams. These earlier laboratory measurements with uniaxial load and only a few in situ measurements were probably made with poor instrumentation as such the results were not generally reliable. The results were used later by others research for determination of the constants and coefficients in the models and for verifying of proposed rheological and temperature models.

Several rheological models have been used to calculate thermal ice pressures, given for the rate of change of the temperature in ice. The laboratory investigations presented after 1968 contained usually tests with both uniaxial and biaxial load. To present the results of the laboratory tests, Lindgren tried to fit the parameters in a linear viscoelastic model composed of a Maxwell and a Kelvin-Voigt element couplet in series. Drouin and Michel (1971) used a nonlinear model considering the number and multiplication rate of dislocations in the ice. For calculation of the temperature profile in the ice for arbitrarily changes of air temperature a graphical variant of Schmidt difference scheme was used in Lundgren model (1964) while the model proposed by Drouin and Michel (1971) predicts rate of temperature increase at various ice depth assuming a sinusoidal temperature rise.

Some of investigators acknowledged that linear viscous-elastic models give an unsatisfactory description of the stress-strain relationship of ice. Bergdahl (1978) proposed a simple nonlinear rheological model composed of a linear spring in series a nonlinear dashpot. The Arrhenius equation was employed to describe the effect of temperature on the creep rate of ice. This model compared to the previously models, appears to best describe the behaviour of ice with the least numbers of unknown parameters and further it was improved by some researchers.

Cox (1984) modified the Bergdahl's (1978) model by introducing a new strain rate function based on the experimental work by Drouin and Michel (1971) which showed a very strong temperature dependence of creep rate, and additionally, a numerical algorithm based on Newton's method was used to solve the nonlinear equation. The proposed rheological model by Fransson (1988) for S1 ice is basically the same as the model by Bergdahl (1978) and Cox (1984). However, one difference is that one empirical constant adjusted to field data.

The differential equation can be solved numerically using a finite difference scheme. However, the lack of an analytical solution of the nonlinear rheological equation is one obstacle that has to be overcome with help of the computer calculations. Another obstacle is that the constants cannot be obtained from simple material tests on the actual ice type passing the transient creep. In this situation it was suggested by Fransson (1988) to use an approximate stress model using the Royen's empirical equation which was expressed in a more general way, with nonlinear dependence of the temperature. In addition, Fransson (1988) proposed a two-step process for determination of the ice pressure. A simple analytical expression was employed for determination of the maximum ice pressure at the centre of ice cove by assuming a nonlinear pressure distribution through the ice. The temperature rise at the centre of the ice was approximated by a straight line.

During several decades the most severe uncertainties about the calculation of ice pressure concern cracks in the ice cover. The methods for calculation of temperature distribution and deformation of the ice could be accurate for an ice cover without cracks. Metge (1976) presented the basic assumptions about cracks in the ice and drew some important conclusion which should be incorporated into the methods for calculating thermal ice pressure. It is still difficult to present how much the calculated maximum pressure should be reduced due to effects of the

dry cracks and/or the weakness of the ice bridges in the wide cracks. However, an attempt to present influence of dry and wide cracks was made by Fransson (1988).

Only some of the proposed models were based on fitting of the field data and were presented as an empirical formula to predict the pressure of ice sheet. Usually these empirical models can require several input parameters. In most situations very limited information is available for the actual ice conditions at the location of the structure. A simple design formula that may serve as guidance for engineers can and should be established for calculation of thermal-induced ice pressure on the structures (Fransson 1988).

Carter et al. (1998) proposed that thermal ice loads are limited by the instability of ice blocks between two or three parallel cracks along a dam wall. Their measurements indicate that the ice pressure changes with increasing water level; the maximum values were about 150 kN/m.

A number of research programs have been conducted over the past 15 years to investigate ice loads on hydro-electric dams. Comfort et al. (1996, 2003) completed an 11 years investigation. Carter et al. carried out measurements as well for Hydro-Québec (Carter et al., 1997, 1998). According to Comfort et al. (2003) the thermal ice load were comprised of two parts: residual load, which are loads that were presented before the start of the loading event and line load increases produced by ice temperature rises, which result from air temperature rises and/or precipitation, particularly snowfalls. Although it was recognized that this approach is not strictly correct from the standpoint of ice rheological behaviour. It was suggested that considerable higher ice loads than traditional values can occur when significant, but not excessive, changes in reservoir levels are expected. The algorithm for calculation of the loads produced by a combination of water level and ice temperature change was presented, and factors controlling the thermal loads are discussed.

In some countries, such as Canada and USA, the recommended thermal ice loads varies between 150 and 220 kN/m depended on ice thicknesses. The values of the thermal ice loads in Sweden depend on the geographical regions and are in the range of 50 and 200 kN/m. The maximum thermal ice pressure of 250 kN/m with ice thickness of 0.6 m has been measured during the laboratory experiment by Löfquist (1952 or 1954) in Sweden.

The values of ice pressure between 150-300 kPa are described in the literature for Russia. However, these values are presented from old sources dated from 1966 - 1970. The values of the thermal and vertical ice loads can be calculated using equations in the Russian standard.

In Norway, the values of the thermal ice loads are between 100 and 150 kN/m. In most cases the value of 100 kN/m (and sometimes lower) can be accepted for calculations for all regions in Norway. However, the measured maximum ice load value was registered as 135 kN/m during the investigation at Silvann dam in the Northern part of Norway. Previously it was suggested, that new measurement programs should be performed in Norway to obtained a better basis for development of the design recommendations, see EBL Kompetanse report (2002). New measurements have been done since 2012 in the Northern Norway. The results showed, that the preliminary calculated line loads are around 100 kN/m und do not exceed a maximum value of 150 kN/m.

The Ice Loads Design Guide with a calculation program (Static Ice Loads On Hydro-Electric Structures 2003) was produced synthesizing the results obtained from various previous years in Canada, and establishing a statistical

database that allows ice loads to be calculated in a coherent format for the long face of dam for various locations, water level change operational regimes, return periods and confidence levels.

Whereas recent studies (Carter et al. 1998 and Comfort et al. 2003) indicate that ice forces could be well above those recommended by the Canadian Dam Association (150kN/m), some public agencies have, in some cases, actually reduced their design values for smaller dams to 100 kN/m. If these dams are truly unsafe, mitigation measures should be defined and applied as soon as possible (Morse et al. 2009). On the other hand, should ice forces not present a safety risk, then investing in dam reinforcement may be a misuse of public funds. Thus, it is important to know what constitutes a safe, realistic and practical design value for ice thrust against linear structures. Due to this need a new project is carried out now in Canada to determine reservoir ice forces on dams.

6. References

AASHTO (1994). American Association of State Highway and Transportation Officials (1994) AASHTO LFRD Bridge Design Specifications, Washington, D. C. 20001.

Ashton, G.D. (1986). River and lake ice engineering, Water Resources Publication, 1986, 485 p.

Assur, A. (1959). Maximum lateral pressure exerted by ice sheets. IAHR VIIth Congress paper 22-SI, Montreal, 1959.

Bergdahl, L. (1978). Thermal Ice pressure in Lake ice cover, Department of Hydraulics, Chalmers University of Technology, Report Series A:2.

Billfalk, L. et al. (1996). Dams and related structures in cold climate - Design guidelines and case studies, Bulletin 105, 1996, ICOLD, 171 s.

Brown, E. and Clarke, G.C. (1932). Ice thrust in connection with hydro-electric plant design. With special reference to the plan at Island Falls on the Churchill River. The Engineering Journal, pp.18-25.

Canadian Department of Environmental (1971). Review of current ice technology and evolution of research priorities. Report series no. 17, Inland Water Branch, Ottawa, Canada.

CAN/CSA-S6-06, Canadian Highway Bridge Design Code S6.1-06. Commentary on CAN/CSA-S6-06, Canadian Highway Bridge Design Code, Rexdale, Ontario, Canada.

Canadian Standards Association (1988). Design of Highway Bridges, National Standard of Canada, CAN/CSA-S6-88, Rexdale, Ontario, Canada.

Canadian Standards Association (2000). Design of Highway Bridges, A National Standard of Canada, CAN/CSA-S6-88, Rexdale, Ontario, Canada.

Carter, D., (2003), “Intensité des poussées statiques excercées par la glace en fonction de l’aire de contact”, Rapport d’étude pour Hydro-Québec, contrat no. 4500542374.

Carter, D.; Sodhi, D.S.; Stander, E.; Caron, O. et Quach, T. (1998). “Ice thrust in reservoirs”.Journal of Cold Regions Sciences and technology, 12(4), p.169-18.

Comfort, G., Gong, Y., Singh, S., and Abdelnour, R. (2003). Static ice loads on dams, Can. J. Civ. Eng. 30(1): 42–68 (2003).

Comfort, G., and Abdelnour, R. (1994). Field measurements of ice loads: Thermal loads on hydroelectric structures, Proceedings, 1994 Canadian Dam Safety Association, Winnipeg, Manitoba, Canada, pp 35–51.

Comfort, G., and Armstrong, T. (2001). Static ice loads on dams: Project update, Canadian Dam Association Bulletin.

Cox, G. (1984). A preliminary investigation of thermal ice pressures. Cold Reg. Science and Technology, 9, pp. 221-229.

Design Criteria for Concrete Arch and Gravity Dams (1977), a Water Resources Technical Publication, Engineering Monograph No. 19, 1977.

Drouin, M. (1970). Sate of Research on ice thermal thrust, IAHR proceedings. Reykjavik, Iceland.

Drouin, M., and Michel, B. (1974). Pressures of Thermal Origin Exerted by Ice Sheets upon Hydraulic Structures, Draft Translation 427, U.S. Army Cold Regions Research and Engineering Laboratory, Hanover, NH.

EBL Kompetanse (2002). Islast mot dammer, Publikasjon nr.: 82-2002 (In Norwegian).

Ekström, T. (2006). A model of ice loads on dam structures. Taylor & Francis Group, pp. 845-850.

Engineering and Design - Ice Engineering (2002). U.S. Army Corps of Engineers EM 1110-2-1612.

Fransson, L. (1988). Thermal Ice Pressure on Structures in Ice Covers, PhD. Thesis 1988:67D, Division of Structural Engineering, Luleå University of Technology.

Gebre, S., Alfredsen, K., Lia, L., Stickler, M., Tesaker, E. (2013). Review of ice effects on hydropower systems. J. Cold Reg. Eng. 27 (4), 196–222.

Gold, L.W. (1958). Some observations on the dependence of strain on stress for ice. Canadian Journal of Physics, Vol. 36, No. 10.

Hassan, P.J. (1991). Thermal ice pressures on dams: a literature review. Ontario Hydro res. Div Report 90-293-K, Toronto, Canada.

Hess, H. (1902).Annalen der Physik, Bd 8, 1902, pp. 405-431, (in German).

Hoseth, K.A. and Fransson, L. (1999). Istrykk på dammer. Måleprogram dam Silvann, vinter 98-99, NVE , nr 21. (In Norwegian).

Jumppanen, P. (1973). Ice thermal loads against wall of water reservoirs, 2:nd Int. Conference on port and Ocean engineering under Arctic Conditions, Reykjavik.

Kjeldgaard, J.H.(1977). Thermal ice forces on hydraulic structures. A short literature review, SINTEFF report No. STF A77043.

Kjeldgaard, J.H., and Carstens, T. (1980). Thermal Ice Forces, in Special Report 80-26, U.S. Army Cold Regions Research and Engineering Laboratory, Hanover, NH, pp 1–33.

Kocahan, H.T. and Rodionov, V.B. (2003), The behaviour fusegates in ice affected environmental, ASDSO-2003.

Kovacs, A. and Sodhi, D.S. (1980). Shore pile-up and ride-up, filed observations, models, theoretical analyses. Cold region science and technology, Vol.2, Elsevier Science Publishers B.V., Amsterdam, The Nederlands, pp 209-288.

Kreüger (1921): Tryckprov av iscuber 15×15×15 from sjöis, Stockholm, 1921.

Lindgren, S. (1968). Istrykk vid temperaturhöjningar. Dept. of Hydraulics, Royal Technical University, Stockholm (In Swedish).

Löfquist (1952, 1954). Studies of the effect of temperature variations, ASCE 2656.

Löfquist, B.(1987). Istryck mot bropelare, Rapport 1987:43, Vägverket (in Swedish).

Mellor, M. (1983). Mechanical behavior of sea ice. CRREL 83-1, US Army Corps of Engineers, Cold regions Research and Engineering laboratory, 102 p.

Metge, M. (1976). Thermal cracks in lake ice. Ph.D. thesis, Queen's University Kingston, Ontario, Canada.

Michel, B. (1970). Ice Pressures on Engineering Structures. Monograph III-B1b, U.S. Army Cold Regions Research and Engineering Laboratory, Hanover, NH.

Michel, B. (1978).Ice Mechanics. Laval University Press, Quebec, PQ, Canada.

Monfore, G.E. and Taylor, F.W. (1948). The Problem of an Expanding Ice Sheet, Proc. Western Snow long, 1948.

Monfore, G.E. (1951). Laboratory investigation of ice pressure, U.S.B.R. Structural Research Laboratory, Report SP-31.

Monfore, G.E. (1952). Ice pressure against dams. Experimental investigation by the Bureau of Reclamation. Proc ASCE, Vol.78, Technical separate No. 162.

Monfore, G.E. (1953). Ice pressure measurements, U.S.B.R. Structural Research Laboratory, Report C-662, 117.

Morse, B., Stander, E., Côté, A., Morse, J., Beaulieu, P., Tarras, A., Noël, P., Pratt, Y. 2009. Ice interactions at a dam face. 15th CRIPE Workshop. St. John's, NFLD.

Morse, B., Stander, E., Côté, A., Martin, R., M. and Desmet, V. (2011).“Stress and Strain dynamics in a hydro-electric reservoir ice sheet”, 16th CRIPE Workshop, Winnipeg,Canada.

Norut Narvik report (2009), Innovativ forvaltning av betongdammer, Report NTAS F2009-1, Norut Narvik, Norway, 2009, 104 p. (in Norwegian).

NVE (2003): Retningslinje for laster og dimensjonering til §§ 4-1 og 4-2 i forskrift om sikkerhet og tilsyn med vassdragsanlegg Norges vassdrags- og energidirektorat, 2003 (In Norwegian).

O'Sadnick, M., C. Petrich, B. Arntsen, and B. Sand (2016). Observations of Ice Stress at Taraldsvikfossen Reservoir, Narvik, Norway. In Proceedings of the 23rd IAHR International Symposium on Ice, Ann Arbor, Michigan, USA, 31 May to 3 June 2016.

P 31.3.07-01 (2001). Guidelines for the calculation of loads and impacts from waves, ships and ice on sea hydraulic engineering constructions, 2001 -P 31.3.07-01. Указания по расчету нагрузок и воздействий от волн, судов и льда на морские гидротехнические сооружения, 2001 (In Russian).

Petrich C and Arntsen B (2018). An overview of trends and regional distribution of thermal ice loads on dams in Norway, ICOLD, 2017.

Petrich C and Arntsen B (2018). An overview of trends and regional distribution of thermal ice loads on dams in Norway, ICOLD, 2017

Petrich, C., I. Sæther, B. Sand, and B. Arntsen (2016). Comparing field data with numerical simulations of ice loads on dams. In Proceedings of the 23rd IAHR International Symposium on Ice, Ann Arbor, Michigan, USA, 31 May to 3 June 2016.

Petrich, C., I. Sæther, L. Fransson, B. Sand, and B. Arntsen (2015). Time-dependent spatial distribution of thermal stresses in the ice cover of a small reservoir. Cold Regions Science and Technology, 120, 35-44.

Petrich, C., I. Sæther, L. Fransson, B. Sand, and B. Arntsen (2014). Preliminary results from two years of ice stress measurements in a small reservoir, In Proceedings of the 22nd IAHR International Symposium on Ice, Singapore, 11–15 August 2014, A. W.-K. Law (ed), NEWRI Nanyang Technological University, Singapore. 452-459.

Proskourjakov (1967). Pression statique de la glace sur les ouvrages hydraulique lors de sa dilatation thermique. Proceedings IAHR XII Congress.

Recommendations on the passage of ice through the hydro-technical structures under building process (2003): (Методические указания по пропуску льда через строящиеся гидротехнические сооружения). СО 34.21.145-2003, VNIIG, St.Petersburg, 2003 (In Russian).

RIDAS – Kraftföretagens riktlinjer för dammsäkerhetsarbete (2008), revidert, Svensk Energi, 2008.

RIL-144 (2001). Guideline for structural loads (in Finnish only), Finnish civil engineers association.

Rose, E. (1947). Thrust exerted by expanding ice sheets, Transactions of the ASCE, 112: 871.

Royen, N. (1922). Istrykk vid temperaturhöjningar. Hyllingsskift tillägnad F. Vilh. Hansen. AB G. Tisells forslag, Stockholm (In Swedish).

Sanderson, T. (1984). Thermal ice forces against isolated structures, Proceedings, IAHR Ice Symposium, Hamburg, Germany, Vol. IV, pp 289–299.

Sanderson, T.J.O. (1988). Ice Mechanics: Risks to Offshore Structures. Graham and Trotman, London.

SN 76-66 (1966). Recommendation on calculation of ice load on river structures (original tittles: Указания по определению ледовых нагрузок на речные сооружения), Russians Standard, 1966 (In Russian).

SNiP II-57-75 (1976). Loads and impacts on Hydraulic structures (from waves, ice and ships) 1976 -Нагрузки и воздействия на гидротехнические сооружения (волновые, ледовые и от судов) SNiP II-57-75, 1976 SNiP II-57-75 (1982). Loads and impacts on Hydraulic structures (from waves, ice and ships)– 1982-Нагрузки и воздействия на гидротехнические сооружения (волновые, ледовые и от судов) SNiP II-57-75, 1982 (In Russian).

SNiP 2.06.04-82* (1982). Loads and impacts on Hydraulic structures (from waves, ice and ships) SNiP 2.06.04-82* - 1982. Нагрузки и воздействия на гидротехнические сооружения (волновые, ледовые и от судов) SNiP 2.06.04-82* (In Russian).

SNiP 2.06.04.82 (1995). Loads and effects on water development works (wave ice and from ships). Нагрузки и воздействия на гидротехнические сооружения (волновые, ледовые и от судов)), Russian national standards, Gosstroy, Moscow, 1995 (In Russian).

SNiP 2.06.04-82*, SP 38.13330.2012 (2014). Loads and impacts on Hydraulic structures (from waves, ice and ships), Нагрузки и воздействия на гидротехнические сооружения (волновые, ледовые и от судов), актуализированная редакция, 2014 (In Russian).

Sodhi, D.S. (1995). Wedging action during vertical penetration of floating ice sheet. Proceedings of Mechanics 95, ASME Publications, New York, pp 65-80.

Sodhi, D.S. (1998). Vertical penetration of floating ice sheets. International Journal of Solids and Structures, 35(31/32), pp 4275-4294.

Sodhi, D.S. and Carter, D. (1998). A model for ice thrust on dam walls. Proceedings of the 14th International Symposium on Ice, Ice in Surface wates, Vol.1, Balkema, Rotterdam, The Nederlands, pp 433-439.

Stander, E. (2006). Ice Stresses in Reservoirs: Effect of Water Level Fluctuations. Journal of Cold Regions Engineering, Vol. 20, No 2, ASCE, ISSN 0887-381X/2006/2-52-67.

Starosolszky, Ö. (1970). Ice in hydraulic engineering, Rapport 70-1, Trondheim , 165 p.

Static Ice Loads On Hydro-Electric Structures (2003) - Summary Report, Ice Load Design Guide, and Ice Load Prediction Computer Program, 2003, report T002700 0206.

Taras, A., Côté, A., Morse, B., Stander, E., Comfort, G., Noel, P., Pratt, Y., and Lupien, R. (2009). “Measurement of Ice Thrust on Dams”. CDA 2009 Annual Conference. Whistler, B.C. Canada, pp 1-12.

Taras, A., Côté, A., Comfort, G., Noel, P., Thériault, L., Morse, B., “Ice thrust measurements at Arnprior and Barrett Chute Dams”, CRIPE 2011, Winnipeg, Canada.

Text STO Gazprom 2-3.7-29-2005 (2005). Method of calculating ice loads on the ice-resistant fixed platform - Текст СТО Газпром 2-3.7-29-2005 Методика расчета ледовых нагрузок на ледостойкую стационарную платформу (In Russian).

Timco, G.W., Watson, D.A., Comfort, G.A. and Abdelnour, R. (1996). A comparison of methods for predicting thermally-induced ice loads, Proceedings 13th IAHR Symposium on Ice, Beijing, China, Vol. 1, pp 241-248.

Tsinker, G.P. (1995). Marine structures engineering: specialized applications Springer, 1995, 548 p.

Water Control Structures Selected Design Guidelines (2004), Alberta Transportation, Transportation & Civil Engineering Division, November 2004.

Xu Bomeng (1981). Pressure due to expansion of ice sheet in reservoirs, IAHR Ice Symposium 1981, Quebec City, pp 540−550.

Xu Bomeng (1986). Design values of pressure due to expansion of ice sheet in reservoir, IAHR Symposium 1986, Iowa City, Iowa, pp 231-238.